

Supporting Information

Demystifying Cp₂Ti(H)Cl and its Enigmatic Role in the Reactions of Epoxides with Cp₂TiCl

Jonathan Gordon,^a Sven Hildebrandt,^b Kendra R. Dewese,^a Sven Klare,^b Andreas Gansäuer,^{*, b}
T. V. RajanBabu^{*,a} and William A. Nugent^{*,a}

- a. Department of Chemistry and Biochemistry, The Ohio State University, 100 West 18th Avenue, Columbus, OH 43210, USA
- b. Kekulé-Institut für Organische Chemie und Biochemie, Universität Bonn, Gerhard-Domagk-Straße 1, 53121 Bonn, Germany

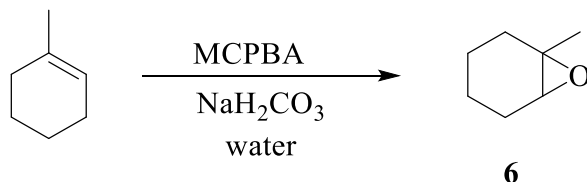
Table of Contents

General Information and Instrumentation.....	S2
Preparation of 1-Methyl-7-oxabicyclo[4.1.0]heptane, 6	S2
Preparation of Authentic Saturated Alcohols <i>cis</i> - 13 and <i>trans</i> - 13	S3
Qualitative and Quantitative Detection of Hydrogen Gas.....	S4
Analysis of Products from Stoichiometric Reactions.....	S5
Isolation of Allylic Alcohols 9a and 9b	S6
GC-MS Analysis of Products from Catalytic Reactions.....	S7
Isotopic Labeling Studies.....	S11
Mechanism of Formation of Cp ₂ Ti(H)Cl.....	S13
Computational Methods.....	S15
Overview of Thermodynamic Data.....	S15
References.....	S21
APPENDIX: Cartesian Coordinates for Optimized Structures.....	S24
Supporting Data: GC, GC-MS and Expanded NMR Traces	S25

General Methods and Instrumentation

Air-sensitive reactions were run under an atmosphere of argon using a Schlenk line or a Vacuum Atmospheres glovebox. THF was distilled over sodium and benzophenone under nitrogen. Other starting materials were obtained from commercial suppliers and used without further purification. Unless otherwise mentioned, ^1H and ^{13}C NMR spectra were recorded at 400 MHz or 100 MHz respectively. Chemical shifts are expressed in parts per million (δ , ppm) using residual solvent signals (CDCl_3) as internal standard. TLCs were run on pre-coated (0.25 mm) silica gel 60 F254 plates from Silicycle. Flash column chromatography was performed over silica gel 40 acquired from Sorbtech Chemicals following a standard protocol.¹ In initial studies, gas chromatograms were obtained on an Agilent HP-5 with a 5%-(Phenyl)-methylpolysiloxane column (30 m x 0.32 mm, 0.25 μm thickness) using hydrogen for the carrier gas. Integrations were obtained using methyl *tert*-butyl ether as an internal standard. Other GC instruments were used for specific applications as described below. Hydrogen was detected on a Shimadzu GC-2014 using a ShinCarbon ST column from Restek. GC-MS studies were carried out on a Shimadzu GCMS-QP2010S chromatograph using a Supelcowax 10 silica coated column (25 μm thickness, 30 m length, 0.25 mm diameter). In situ IR studies were carried out using a ReactIR-15 instrument manufactured by Mettler Toledo.

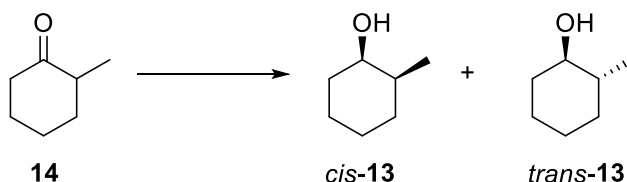
Preparation of 1-Methyl-7-oxabicyclo[4.1.0]heptane, **6** (Equation S1)



Equation S1

Epoxide **6** was prepared using a minor modification of the procedure of Franguelli.² 1-Methylcyclohexene (2.44 g, 25.4 mmol, 3.0 mL) was added to a solution of sodium hydrogen carbonate (8.50 g, 101 mmol) in water (340 mL) and the mixture was cooled to 0 °C. 3-Chloroperoxybenzoic acid (8.76 g, 77% purity, 39.0 mmol) was added in portions with stirring. The mixture was allowed to warm to room temperature with continued stirring overnight. The product was extracted into diethyl ether (3 x 200 mL). After distillation of the solvent at reduced pressure, the crude epoxide was subjected to flash chromatography on silica (95:5 pentane/diethyl ether). Distillation of the solvent at reduced pressure afforded **6** (1.20 g, 42%) as a colorless liquid. ^1H NMR (400 MHz, CDCl_3) δ 2.94 (d, 1H, J = 3.3 Hz), 1.82-1.91 (m, 3H), 1.62-1.70 (m, 1H), 1.37-1.44 (m, 2H), 1.28 (s, 3H, J = 0.9 Hz), 1.15-1.45 (m, 2H). ^{13}C NMR (100 MHz, CDCl_3) δ 59.6, 57.4, 29.9, 24.7, 23.9, 20.0, 19.6. GC-MS (5% phenyl methyl silicone, 35 °C, R_t = 8.78 min) m/z 112.10 ($[\text{M}^+]$); calcd for $\text{C}_7\text{H}_{12}\text{O}$ 112.09. Spectral data match those reported in the literature.^{3,4}

Preparation of Authentic Saturated Alcohols *cis*-10 and *trans*-10 (Equation S2)



Equation S2

Solution of 2-methylcyclohexanone (0.60 mL, 0.56 g, 5.0 mmol) in ethanol (10 mL) was cooled to 0 °C. Sodium borohydride (0.28 g, 7.5 mmol) was added over the course of several minutes at room temperature and the mixture was stirred for 24 h. The ethanol was evaporated and saturated aqueous NH₄Cl (10 mL) was added. The mixture was extracted into diethyl ether (3 x 10 mL) and the combined organic extracts were washed with brine and dried over Na₂SO₄ at which point GLC indicated the formation of *cis*-13 and *trans*-13 in a ratio of *cis/trans* = 42:58. The solvent was distilled off at reduced pressure to afford 0.495 g (87%) of crude residue containing the mixed alcohols. The isomers were separated by flash chromatography in 20:1 pentane/ether. Comparison of the ¹H NMR spectra of the isolated products with those in the literature⁵ indicated that the first eluting isomer is *cis*-13 and the later eluting isomer is *trans*-13. Spectra are shown below as Figure S1 and Figure S2 respectively.

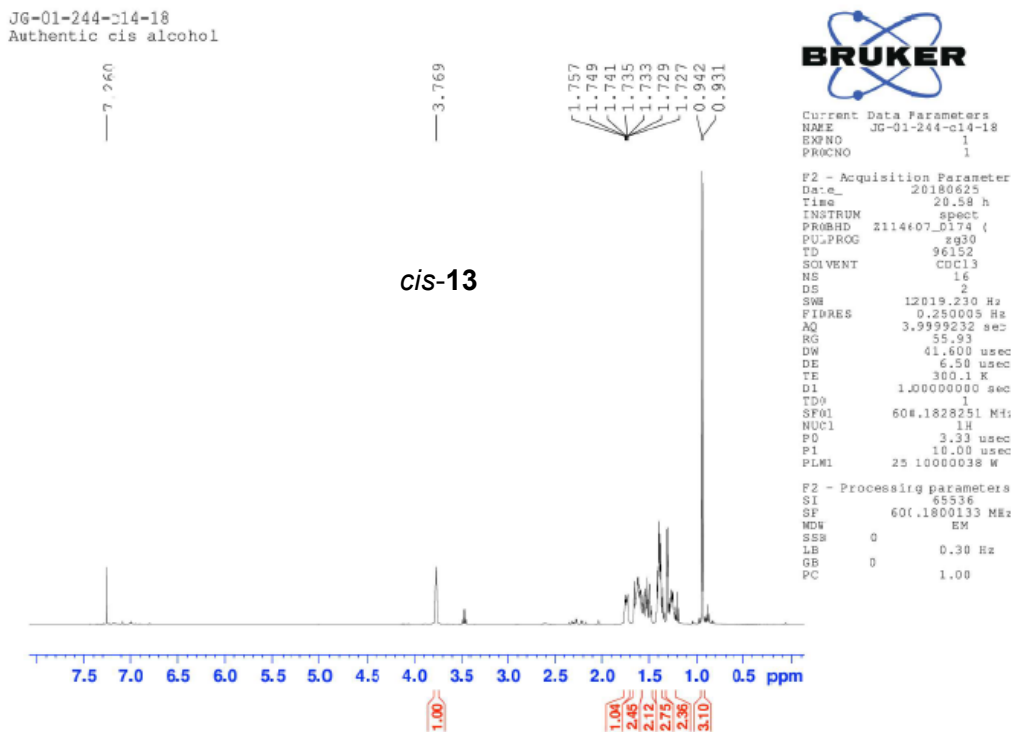


Figure S1. ¹H NMR of authentic *cis*-13 in CDCl₃.

JG-01-244-c21-28
authentic *trans* alcohol

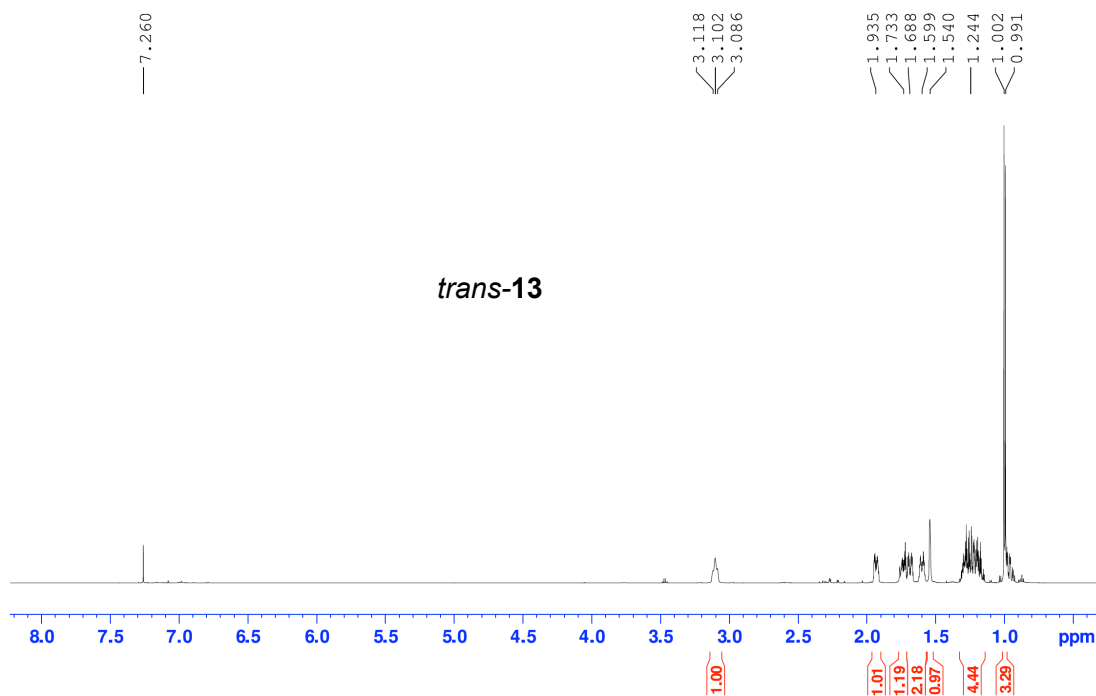


Figure S2. ^1H NMR of authentic *trans*-13 in CDCl_3 .

Qualitative and Quantitative Detection of Hydrogen Gas.

Titanocene dichloride (0.498 g, 2.00 mmol) and zinc dust (0.393 g, 6.00 mmol) were placed in a Schlenk flask which was then flushed with argon. To the flask were added THF (6.0 mL) and *tert*-butyl methyl ether (238 μL , 0.177 g, 2.00 mmol) as an internal standard. The mixture was stirred for 30 minutes at which time the initial red color had discharged to lime green. The flask was closed to argon and a thin tube was fed from the flask into an inverted burette filled with water (see Figure S3 below). A solution of epoxide (0.225 g, 2.00 mmol) in 1.5 mL of THF was added slowly and as gas evolved, it bubbled into the burette to displace 22.4 mL of water.

The gas was identified as hydrogen via gas chromatography. This was accomplished by analysis of the headspace above the reaction on a Shimadzu GC-2014 instrument equipped with a ShinCarbon ST column. It was also possible to confirm the yield of hydrogen gas observed in

the gas burette experiments using a calibration curve. In all cases the yield of H₂ conformed ($\pm 10\%$) to the formulation in which 2 allylic alcohol \rightarrow 1 H₂.

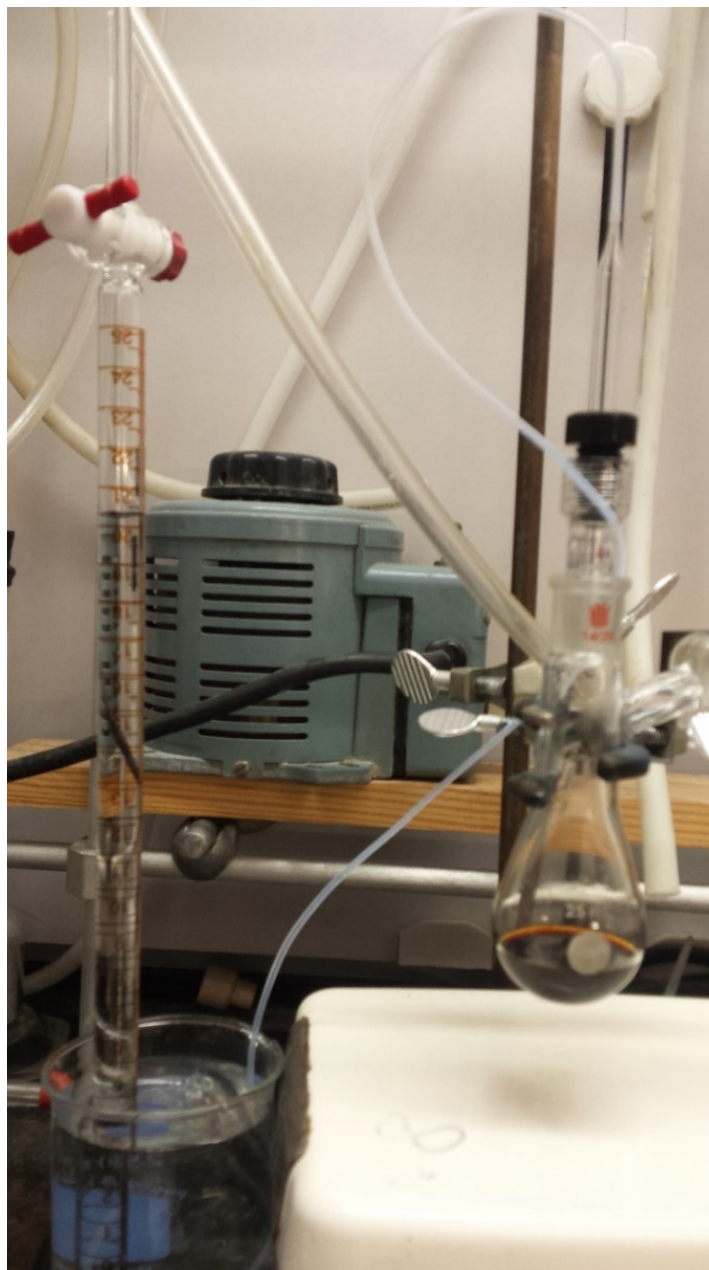


Figure S3. Set-up for Gas Burette Experiments.

Analysis of Products from Stoichiometric Reaction of 6 with Cp₂TiCl.

When the reaction of epoxide **6** with Cp₂TiCl was carried out as described in the Experimental Section, the principal products were the allylic alcohols **9a** and **9b**. A typical GLC trace of the

crude product is shown in Figure S4 and the ^1H NMR of crude product after removal of solvent is shown in Figure S5.

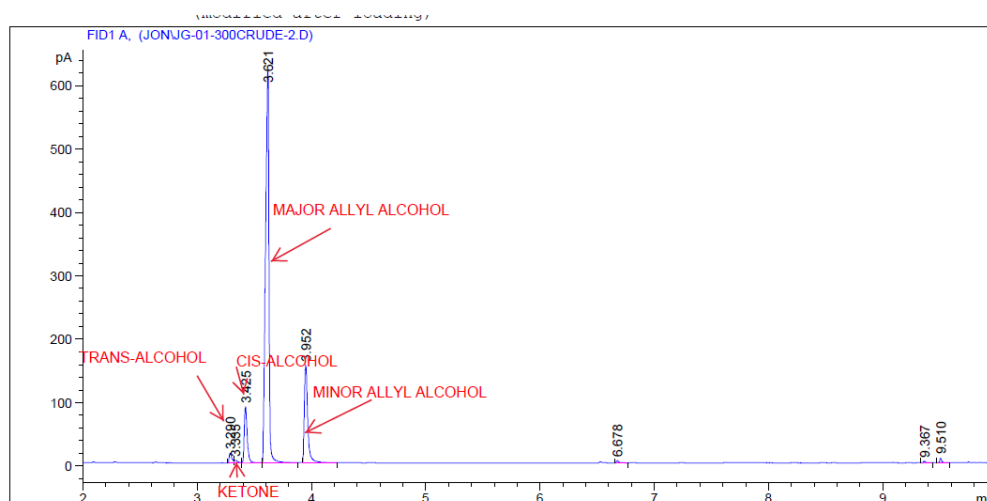


Figure S4. Gas Chromatographic Analysis (5%-phenyl)methylsilicone) of Reaction of 1-Methyl-1,2-epoxycyclohexane and Stoichiometric Cp_2TiCl .

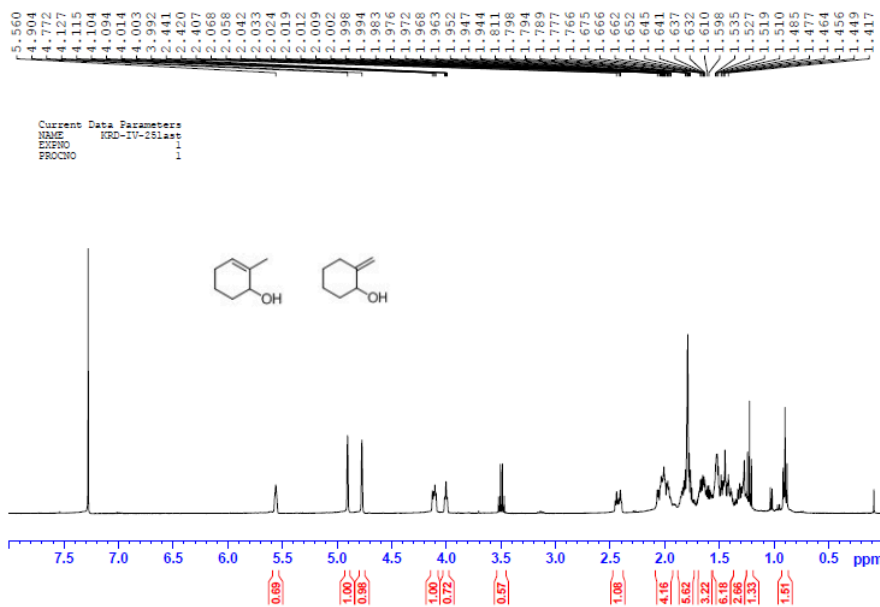
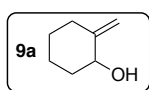


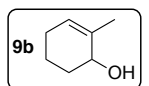
Figure S5. ^1H NMR of Crude Product (in CDCl_3) from Reaction of 1-Methyl-1,2-epoxycyclohexane and Stoichiometric Cp_2TiCl .

Isolation of Allylic Alcohols 9a and 9b.

In order to confirm the identity of **9a** and **9b** and to enable preparation of a GC calibration curve, the allylic alcohols were isolated by flash chromatography. It was not possible to separate the regioisomers chromatographically; instead, fractions were collected so as to provide a sample that was relatively enriched in the minor regioisomer. The above reaction mixture was quenched with 2.5 mL of saturated aqueous sodium hydrogen carbonate. Prior to flash chromatography, gas chromatographic analysis indicated the formation of allylic alcohols **9a** and **9b** (1.88 mmol total) in a 5:1 ratio. The response factors for **9a** and **9b** were presumed to be identical. The solution was filtered over Celite, rinsing with THF, and was subjected to flash chromatography (4:1 pentane/diethyl ether) to obtain a 2:1 mixture of 2-methylenecyclohexan-1-ol **9a** (major) and 2-methylcyclohex-2-ene-1-ol **9b** (minor) as a yellow oil (63 mg). NMR analysis and comparison with literature data^{6,7} allowed the assignment of the spectra as follows.



For the major product **9a**: ¹H NMR (400 MHz, CDCl₃) δ 4.90 (s, 1H), 4.77 (s, 1H), 4.09-4.13 (m, 1H), 2.41-2.45 (m, 1H), 1.94-1.53 (m, 8H); ¹³C NMR (100 MHz, CDCl₃) δ 151.6, 105.0, 72.7, 36.7, 33.5, 27.7, 23.8 GC-MS (5%-phenylmethyl silicone, 35 °C for 10 min then ramp at 20 °C/min, R_t = 12.12 min) *m/z* 112.10 ([M+]); calcd for C₇H₁₂O 112.09. NMR data are essentially identical to those in the literature.⁶



For the minor product **9b**: ¹H NMR (400 MHz, CDCl₃) δ 5.56 (br s, 1H), 4.00 (t, *J* = 4.4 Hz, 1H), 2.1-1.5 (m, 7H), 1.76 (d, *J* = 1.9 Hz, 3H); ¹³C NMR (100 MHz, CDCl₃) δ 135.3, 125.5, 68.5, 32.2, 25.4, 20.6, 18.1; GC-MS (5% phenylmethyl silicone, 35 °C for 10 min then ramp at 20 °C/min, R_t = 12.40 min) *m/z* 112.10 ([M+]); calcd for C₇H₁₂O 112.09. NMR data are essentially identical to those in the literature.⁷

GC-MS Analysis of Products from Catalytic Reactions

Additional side-products were observed under catalytic conditions, namely the reduction product *cis*- and *trans*-**13** and the ketone **14**. In order to determine the yield of these products, this portion of the study utilized a different GC column (Supelcowax 10), which did not allow separation of the regioisomers of allylic alcohol **9**. However, the ratio of **9a** to **9b** was separately determined by examination of the vinylic region of the crude ¹H NMR spectrum. See Figure S8 below.

In a Schlenk tube, 2,4,6-collidinium chloride (1.50 eq) is sublimed *in vacuo* under careful heating. The solids are flushed with argon after cooling to room temperature and transferred back to the bottom of the flask. Zn powder (3.00 eq) and Cp₂TiCl₂ (0.05 to 1.00 eq) are added and the solids are evacuated and flushed with argon three times. Dry THF (substrate 0.25 M) is added via syringe and the reaction is stirred for 15 minutes at room temperature. The solution turns green within minutes. 1,2-Epoxy-1-methylcyclohexane (1.00 eq) is added via syringe and the reaction is stirred under argon at room temperature for the indicated time. Saturated aqueous NH₄Cl solution is added (100% v/v THF) and the aqueous phase is extracted with ethyl acetate three times. The combined yellow organic phase is filtered through a short silica pad. The solvent is removed under reduced pressure (not below 150 mbar at 40 °C, due to volatility of the substrate and products) to yield the crude product that is subjected to GC-MS analysis.

GC-MS conditions:

GC-MS: Shimadzu GCMS-QP2010S.

Column: Supelcowax 10 silica coated column; 25 μm thickness, 30 m length, 0.25 mm diameter.

Sample preparation: A fraction of the crude product or the reaction solution is dissolved in *n*-hexane and injected into the GC-MS.

Method: Injection temp.: 250 $^{\circ}\text{C}$, Oven temp.: 10 min @ 40 $^{\circ}\text{C}$, then 40 to 200 $^{\circ}\text{C}$ @ 10 $^{\circ}\text{C}/\text{min}$, then 10 min @ 200 $^{\circ}\text{C}$, Column flow rate: 0.73 mL/min, Carrier gas: He.

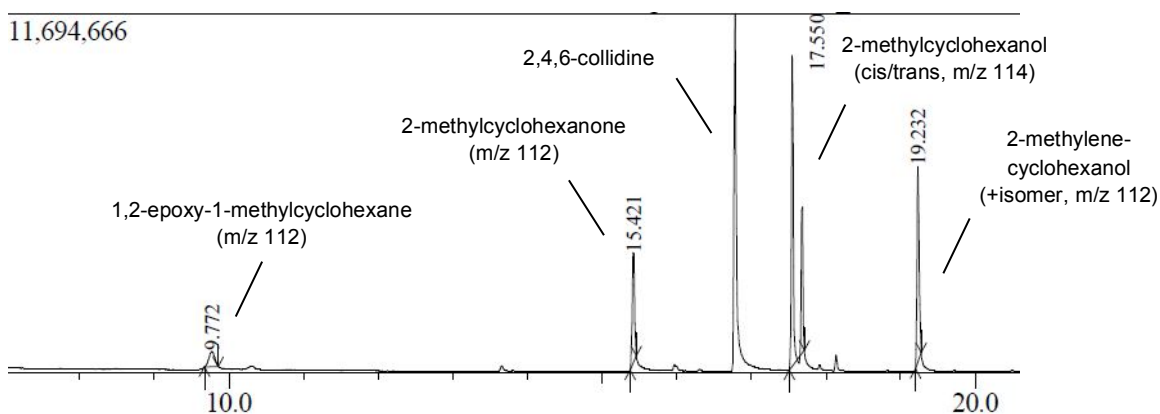
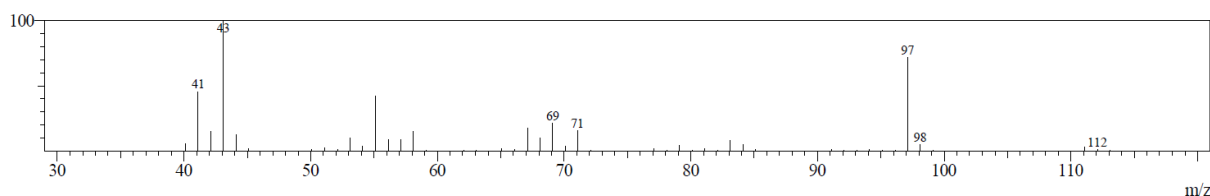
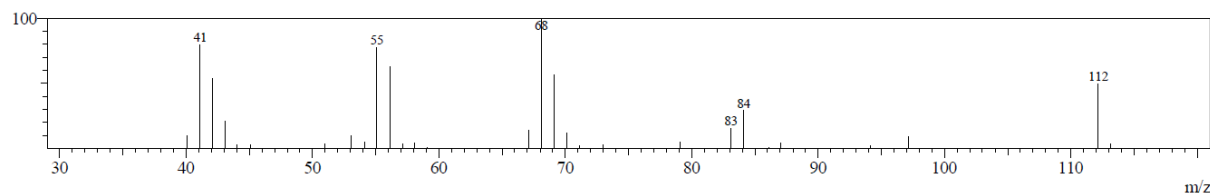


Figure S6. Representative GC-MS trace of a catalytic reaction with incomplete conversion.

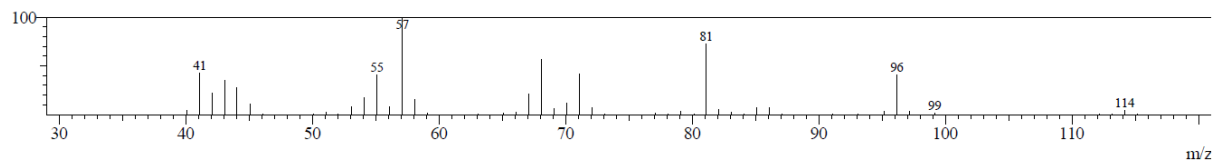
1,2-epoxy-1-methylcyclohexane (**6**): Retention time: 9.8 min



2-methylcyclohexanone (**14**): Retention time: 15.4 min



cis/trans-2-methylcyclohexanol (**13**): Retention time: 17.6, 17.7 min



Allylic alcohols (**9a** and **9b**): Retention time: 19.2 min

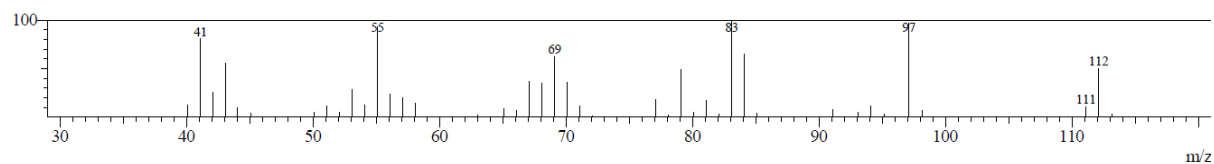


Figure S7. Mass spectra (EI) observed during GC-MS experiments.

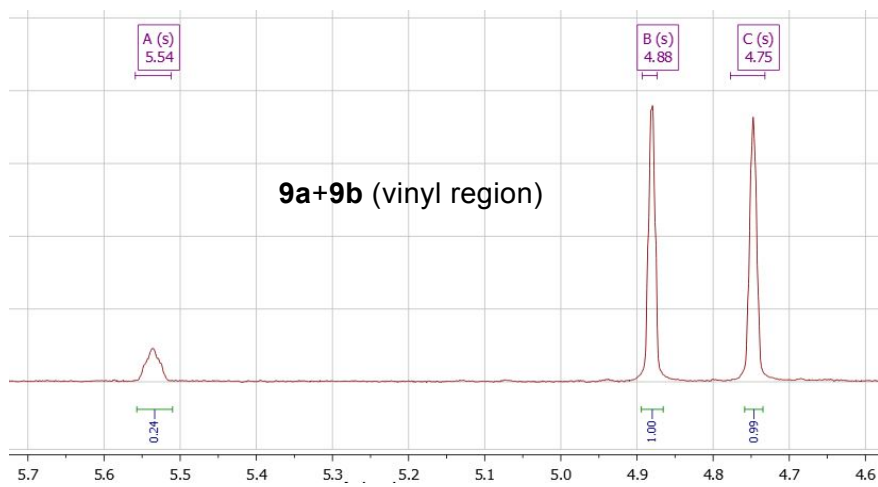
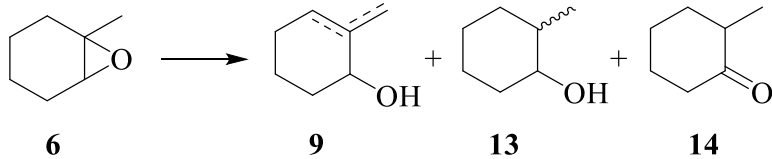
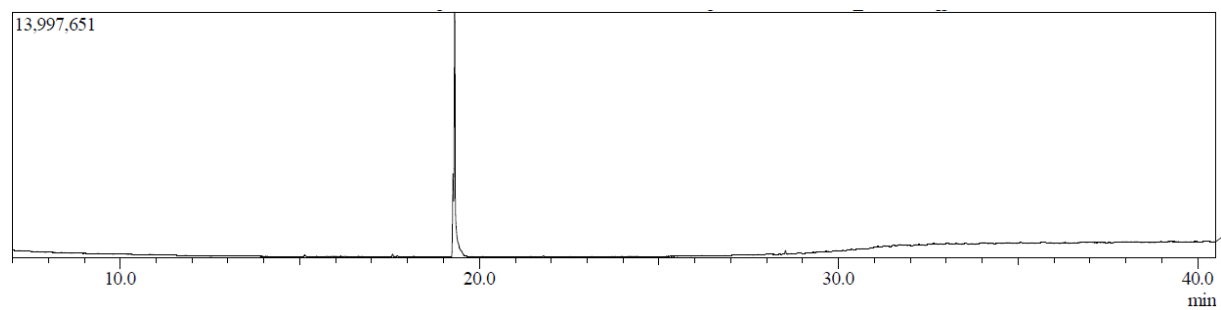


Figure S8. Crude ^1H NMR of vinylic region (δ 4.6-5.7) for allylic alcohols **9a** and **9b** in CDCl_3 .

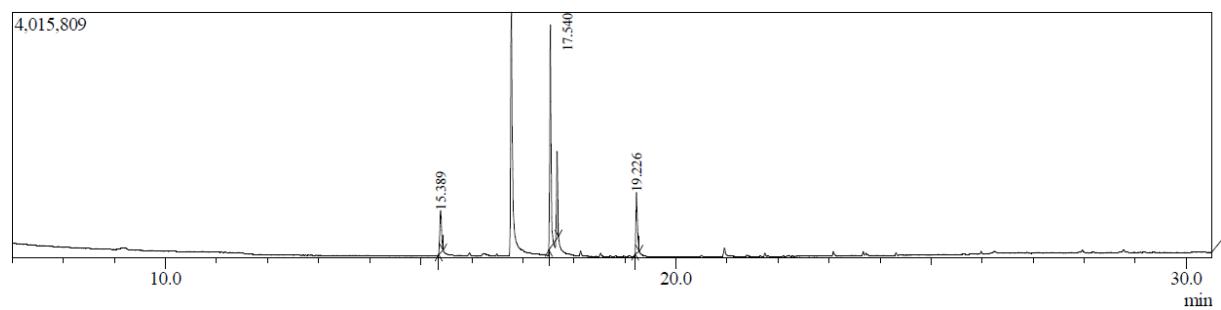


(Cp ₂ TiCl ₂ /Zn/Coll•HCl), THF, 20 h, RT, 0.25 M		6	9	13	14
1	1 eq / 3 eq / -, 15 mins, gas evol.	-	100	-	-
2	5 mol% / 3 eq / 1.5 eq	-	11	70	19
3	25 mol% / 3 eq / 1.5 eq	-	44	53	3
4	25 mol% / 3 eq / 1.5 eq, Et ₂ O, 2.5 h	-	71	24	5
5	25 mol% / 3 eq / 1.5 eq, PhMe	-	67	24	9

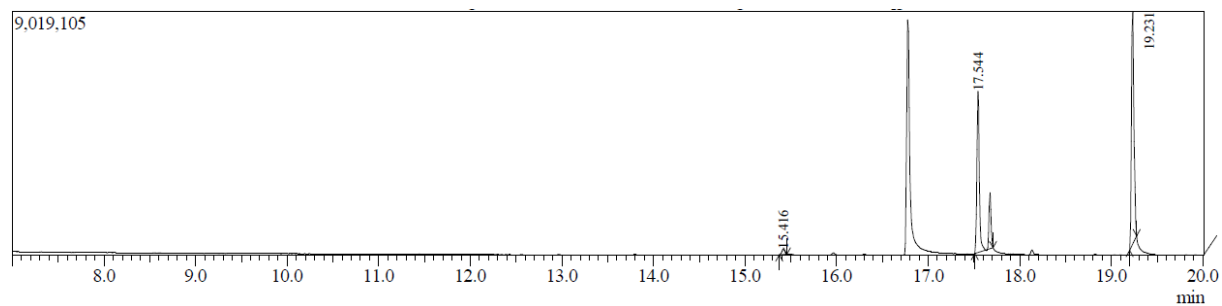
Entry 1:



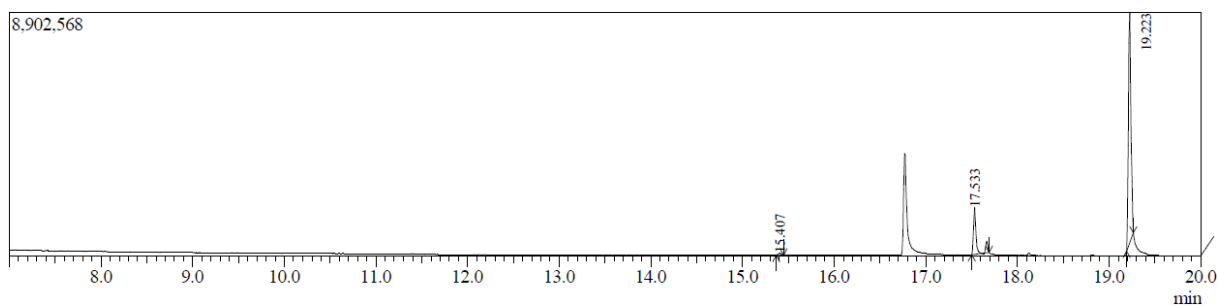
Entry 2:



Entry 3:



Entry 4:



Entry 5:

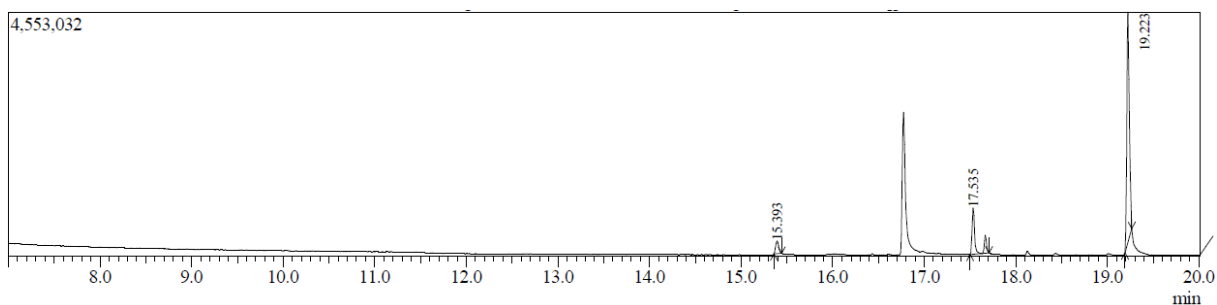


Figure S9. GC-MS traces of selected experiments

Isotopic Labeling Studies

Reactions were run as described in the Experimental Section of manuscript. The more abundant *cis*-**13** isomer of the saturated alcohol was selected for study. GC-MS conditions were as follows:

GC-MS conditions:

MS: Agilent Technologies 5975 series MSD (electron impact ionization)

GC: Agilent Technologies 6850 network GC system

Capillary Column: HP-5MS (5%-Phenyl)methyl Siloxane

Dimensions: 30 m length; 250 μm diameter; 0.25 μm film thickness

Sample Prep: A fraction of the crude product or reaction solution is dissolved in 1:1 n-hexane: diethyl ether and injected into the GC-MS

Method: Injection Temp.: 250°C, Oven temp.: 5 min @ 35°C, then 35°C to 250°C @ 5°C/min, then 2 min at 250°C; Column Flow Rate 2.3 mL/min; Carrier gas: He

The relative intensity for the M and M+1 peaks was determined by integrating the total ion current for the *cis*-**13** molecular ion (retention time ~ 10. 2-10.3 min) at m/Z = 114 and 115. The resulting ratios were corrected for 0.078% contribution from the naturally occurring isotopes ¹³C and ²H. Shown in the following pages are results for authentic (unlabelled) *cis*-**13** and various samples of *cis*-**13** obtained from reactions of **6** done with coll.HCl and coll.DCl in THF or THF-d₈ as outlined in Table 4.

DATA FOR TABLE 4 (in Publication) [See pages S26-37]

Entry 1. Authentic *cis*-**13**

GC

¹H NMR

GC-MS showing [M+], [M+1] and [M+]/[M+1]

Entry 2. *cis*-**13** prepared using coll.HCl and THF-d₈

GC-MS showing [M+], [M+1] and [M+]/[M+1]

Entry 3. *cis*-**13** prepared using coll.DCl and THF

GC-MS showing [M+], [M+1] and [M+]/[M+1]; [M+2]

Entry 4. (*Run in duplicate*) *cis*-**13** prepared using coll.DCl and THF-d₈

GC-MS showing [M+], [M+1] and [M+]/[M+1]; [M+2]

The location of the isotopic label in *cis*-**13** produced in the isotopic labeling experiments was confirmed to be the tertiary (methyl bearing) carbon using 600 MHz ^1H NMR (see also, Figures S12-14). The resonance for the tertiary hydrogen was located using a combination of COSY, HSQC, and 1D-decoupling and appears as a multiplet in the δ 1.61-1.64 region. The tertiary hydrogen resonance itself is poorly resolved due to overlapping resonances, which interfere with integration. However, the associated methyl resonance is more useful. In protio-*cis*-**13** the methyl group appears as a doublet ($J = 6.8$ Hz) at δ 0.94 ppm (upper spectrum Figure S10). Superimposed on the methyl doublet in this spectrum is the methyl singlet for deuterium labeled *cis*-**13**, which exhibits the expected⁸ upfield isotopic shift to 0.93 ppm. In the lower spectrum, irradiation of the 3° hydrogen at δ 1.614 collapses the methyl doublet to a singlet so that the two methyl singlets are now resolved.

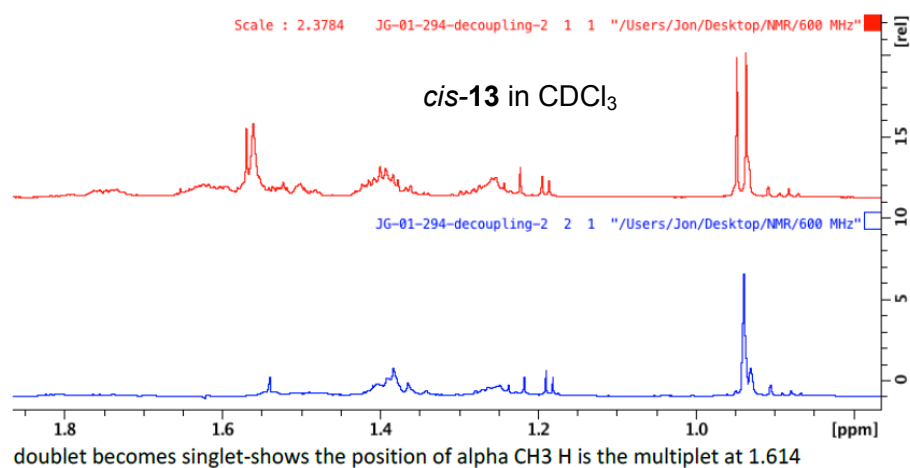
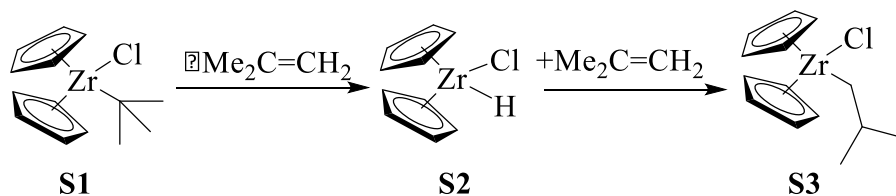


Figure S10. ^1H NMR spectra (in CDCl_3) showing the effect of irradiation of 3° hydrogen at δ 1.614 ppm.

Mechanism of $\text{Cp}_2\text{Ti}(\text{H})\text{Cl}$ formation.

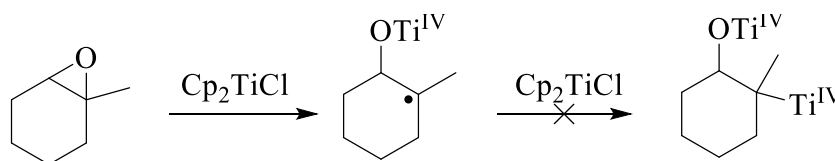
Two different mechanisms have been proposed for the formation of $\text{Cp}_2\text{Ti}(\text{H})\text{Cl}$ when Cp_2TiCl reacts with tertiary alkyl radicals. Here we briefly review the evidence for each.

One proposed mechanism involves the combination of the 3° β -titanoxy radical with Cp_2TiCl to afford a 3° titanium(IV) organometallic which next undergoes β -hydride elimination.^{9,10} Analogy can be drawn to the well-known instability of 3° zirconium(IV) organometallics (Scheme S1). When *tert*-butyl zirconocene complex **S1** is generated by treatment of Cp_2ZrCl_2 with *t*-BuLi or *t*-BuMgCl at low temperature and is allowed to warm to room temperature, the isobutyl complex **S3** is isolated.^{11,12} The reaction proceeds by β -hydride elimination of isobutylene affording Schwartz's reagent (**S2**), followed by re-addition of isobutylene to afford **S3**.



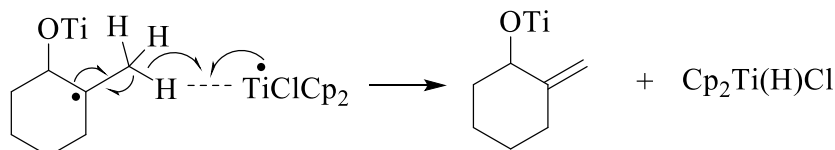
Scheme S1 . Reaction of (t-butyl)zirconocene chloride

In the other model, the 3° β -titanoxy radical is not trapped as an organotitanium compound.¹³ This is consistent with kinetic evidence that a bulky 3° radical is not able to efficiently form a Ti–C bond for steric reasons (Scheme S2).¹⁴



Scheme S2 . Epoxide opening by Cp_2TiCl

Instead, the carbon-centered radical and the titanium-centered radical reacts by a “mixed disproportionation” process (Scheme S3).¹³ When, as in Scheme S3, one of the substituents on a 3° β -titanoxy radical is a methyl group, the hydrogen atom is principally lost from the methyl group. Abstraction of the methyl hydrogen may be preferred for both steric and stereoelectronic reasons.¹⁵ The former is related to steric accessibility of the primary hydrogens, while the latter reflects free rotation of the methyl substituent which facilitates orbital overlap between the C–H bond of the methyl group and the semi-filled p orbital of the radical center.



Scheme S3. Mechanism of β -hydrogen abstraction by Cp_2TiCl

Regardless of which mechanism is responsible for the loss of β -hydrogen, β -hydride elimination or mixed disproportionation, the titanium containing product is titanocene hydrido-chloride and the conclusions regarding the thermal instability of $\text{Cp}_2\text{Ti}(\text{H})\text{Cl}$ would not be affected.

Computational Methods

TURBOMOLE 7.0 was used for quantum chemical calculations.¹⁶ Geometries were optimized on the DFT level using the TPSS density functional¹⁷ together with Ahlrichs' polarized triple-zeta Gaussian AO basis set def2-TZVP¹⁸, avoiding major BSSE effects without employing counterpoise corrections.

For all DFT calculations the resolution-of-the-identity (RI) approximation for the Coulomb integrals¹⁹ with matching default auxiliary basis sets²⁰ was applied. The numerical quadrature grid m4 was employed for integration of the exchange-correlation contribution during geometry optimizations. Default settings for convergence criteria of energy and gradients were not changed. For all geometry optimizations and single point calculations, Grimme's D3 dispersion correction scheme²¹ together with the Becke-Johnson (BJ) damping²² was applied. For a detailed description of the dispersion correction, see ref. 23; for recent chemical applications of Grimme's D3 correction, see e.g. ref. 24.

The rovibrational corrections from energy to the free energy were obtained by a modified rigid-rotor-harmonic-oscillator statistical treatment²⁵ based on analytical harmonic frequencies calculated on the TPSS-D3/def2-TZVP level. For the entropy calculation, frequencies with wavenumbers below 100 cm^{-1} were treated as rigid rotors to avoid inherent errors in the harmonic approximation. Artificial small frequency imaginary modes of up to $i10\text{ cm}^{-1}$ were inverted and included into the enthalpy and entropy calculations.

Solvent effects on the thermochemical properties were taken into account by the COSMO-RS model²⁶ used as implemented in COSMOtherm²⁷ to obtain all solvation free energies. Single point calculations employing the default BP86²⁸/def-TZVP¹⁸ level of theory were performed on the optimized geometries. Solvation contributions to free energies at 298.15 K for THF were computed for these gas phase structures.

Single point energies were obtained in the gas phase on the PW6B95-D3²⁹ or B3LYP³⁰/D33 level together with the large quadruple-zeta basis set def2-QZVP³¹ and the larger grid m5 which should guarantee converged single-point energies.

OVERVIEW OF THERMODYNAMIC DATA

In the tables that follow, energies are given in $\text{kcal}\cdot\text{mol}^{-1}$. Solvation contributions to free energies at 298.15 K were calculated for THF.

Table S1. Calculated thermodynamic parameters for H₂ generation from (C₅R₅)₂TiHCl

(C ₅ R ₅) ₂ TiHCl		→	(C ₅ R ₅) ₂ TiCl + 1/2 H ₂		
			ΔE	ΔG	ΔG_{solv}
Cp₂TiHCl	B3LYP-D3		- 3.25	- 8.95	- 8.62
	PW6B95-D3		- 4.00	- 9.70	- 9.37
(C₁C₅H₄)₂TiHCl	B3LYP-D3		- 4.25	- 10.06	- 11.06
	PW6B95-D3		- 5.12	- 10.93	- 11.93
Cp*₂TiHCl	B3LYP-D3		- 2.68	- 8.77	- 7.96
	PW6B95-D3		- 3.36	- 9.45	- 8.63

Table S2. Calculated thermodynamic parameters for H₂ generation from (C₅R₅)₂TiHCl in THF

(C ₅ R ₅) ₂ TiHCl + THF		→	(C ₅ R ₅) ₂ TiCl*THF + 1/2 H ₂		
			ΔE	ΔG	ΔG_{solv}
Cp₂TiHCl	B3LYP-D3		- 15.25	- 6.60	- 10.50
	PW6B95-D3		- 16.30	- 7.65	- 11.55
(C₁C₅H₄)₂TiHCl	B3LYP-D3		- 16.25	- 7.52	- 11.67
	PW6B95-D3		- 17.03	- 8.30	- 12.45
Cp*₂TiHCl	B3LYP-D3		- 7.54	2.19	- 0.04
	PW6B95-D3		- 8.64	1.09	- 1.15

Table S3. Calculated thermodynamic parameters for metathesis between Cp₂TiHCl and TMSCl

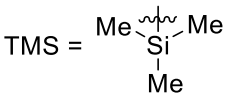
$\text{Cp}_2\text{TiHCl} + \text{TMSCl} \longrightarrow \text{Cp}_2\text{TiCl}_2 + \text{TMSH}$			
TMS = 			
	ΔE	ΔG	ΔG_{solv}
B3LYP-D3	- 2.96	- 1.45	- 3.28
PW6B95-D3	- 1.68	- 0.18	- 2.00

Table S4. Calculated thermodynamic parameters for reaction between Cp₂TiHCl and Me•

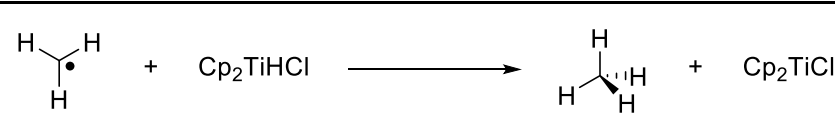
			
	ΔE	ΔG	ΔG_{solv}
B3LYP-D3	- 59.15	- 54.73	- 57.49
PW6B95-D3	- 62.30	- 57.88	- 60.64

Table S5. Calculated thermodynamic parameters for reaction between Cp₂TiHCl and (Me)₃C•


			
	ΔE	ΔG	ΔG_{solv}
B3LYP-D3	- 48.32	- 43.72	- 44.43
PW6B95-D3	- 50.83	- 46.22	- 46.93

Table S6. Calculated thermodynamic parameters for disproportionation reaction between Cp_2TiHCl and 1-methyl-2-methoxy cyclohexyl radical

	ΔE	ΔG	ΔG_{solv}
B3LYP-D3	- 51.67	- 47.40	- 46.86
PW6B95-D3	- 54.28	- 50.01	- 49.47

Table S7. Calculated thermodynamic parameters for disproportionation reaction between Cp_2TiHCl and 1-methyl-2-(*bis*-cyclopentadienyl)(chloro)titanoxy cyclohexyl radical

	ΔE	ΔG	ΔG_{solv}
B3LYP-D3	- 49.47	- 45.54	- 45.11
PW6B95-D3	- 52.47	- 48.54	- 48.11

Table S8. Calculated thermodynamic parameters for H-abstraction reaction from ethyl radical by Cp_2TiCl

	ΔE	ΔG	ΔG_{solv}
B3LYP-D3	- 9.01	- 8.31	- 9.68
PW6B95-D3	- 8.85	- 8.15	- 9.52

Table S9. Calculated thermodynamic parameters for H-abstraction reaction from 2-methoxy-1-methyl cyclohexyl radical by Cp₂TiCl

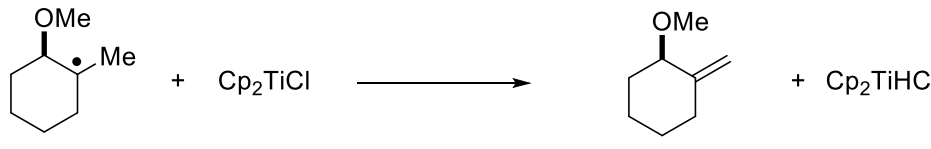
	ΔE	ΔG	ΔG_{solv}
B3LYP-D3	-11.00	- 10.51	- 11.46
PW6B95-D3	-10.72	- 10.23	- 11.18

Table S10. Calculated thermodynamic parameters for β -H-abstraction reaction (from Me) from 1-methyl-2-(bis-cyclopentadienyl)(chloro)titanoxy cyclohexyl radical by Cp₂TiCl

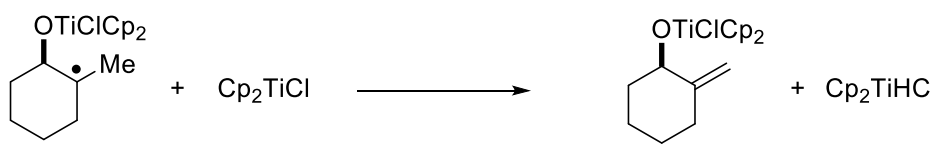
	ΔE	ΔG	ΔG_{solv}
B3LYP-D3	- 9.70	- 9.30	- 10.19
PW6B95-D3	- 9.95	- 9.55	- 10.44

Table S11. Calculated thermodynamic parameters for β -H-abstraction reaction (from CH_2) from 1-methyl-2-methoxy cyclohexyl radical by Cp_2TiCl

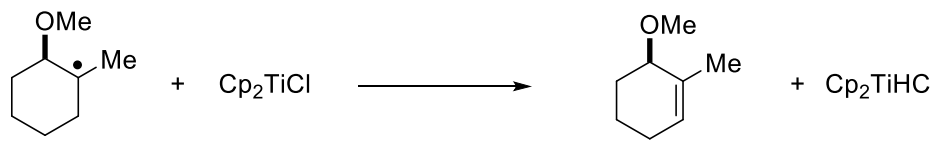
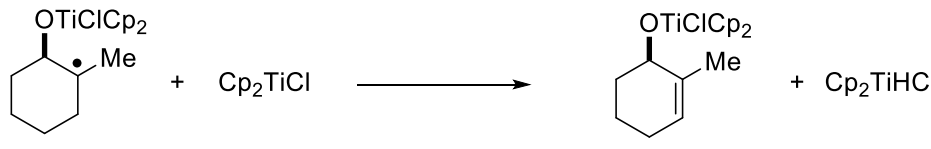
	ΔE	ΔG	ΔG_{solv}
B3LYP-D3	- 12.93	- 12.99	- 13.64
PW6B95-D3	- 12.87	- 12.93	- 13.58

Table S12. Calculated thermodynamic parameters for β -H-abstraction reaction (from CH_2) from 1-methyl-2-(bis-cyclopentadienyl)(chloro)titanoxy cyclohexyl radical by Cp_2TiCl

	ΔE	ΔG	ΔG_{solv}
B3LYP-D3	- 11.12	- 11.58	- 12.33
PW6B95-D3	- 11.25	- 11.71	- 12.46

References

- (1) Still, W. C. Rapid chromatographic technique for preparative separations with moderate resolution. *J. Org. Chem.* **1978**, *43*, 2923-2925.
- (2) Franguelli, F.; Germani, R.; Pizzo, F.; Savelli, G. Epoxidation reaction with *m*-chloroperoxybenzoic acid in water. *Tetrahedron Lett.* **1989**, *30*, 1427-1428.
- (3) Tse, M. K.; Klawonn, M.; Bhor, S.; Döbler, C.; Anilkumar, G.; Hugl, H.; Mägerlein, W.; Beller, M. Convenient method for epoxidation of alkenes using aqueous hydrogen peroxide. *Org. Lett.* **2005**, *7*, 987-990.
- (4) Kon, Y.; Ono, Y.; Matsumoto, T.; Sato, K. An effective catalytic epoxidation of terpenes with hydrogen peroxide under organic solvent-free conditions. *Synlett* **2009**, 1095-1098.
- (5) Wiitala, K. W.; Al-Rashid, F. Z.; Dvornikovs, V.; Hoye, T. R.; Cramer, C. J. Evaluation of various DFT protocols for computing ¹H and ¹³C chemical shifts to distinguish stereoisomers: diastereomeric 2-, 3-, and 4-methylcyclohexanols as a test case. *J. Phys. Org. Chem.* **2007**, *20*, 345-354.
- (6) Schomaker, J. M.; Pulgam, V. R.; Borhan, B.V. Synthesis of diastereomerically and enantiomerically pure 2,3-disubstituted tetrahydrofurans using a sulfoxonium ylide. *J. Am. Chem. Soc.* **2004**, *126*, 13600-13601.
- (7) Lhermet, R.; Durandetti, M.; Maddaluno, J. Intramolecular carbonickelation of alkenes. *Beilstein J. Org. Chem.* **2013**, *9*, 710-716.
- (8) O'Leary, D. J.; Allis, D. G.; Hudson, B. S.; James, S.; Morgera, K. B.; Baldwin, J. E. Vicinal Deuterium Perturbations on Hydrogen NMR Chemical Shifts in Cyclohexanes. *J. Am. Chem. Soc.* **2008**, *130*, 13659-13663.
- (9) Bermejo, F.; Sandoval, C. Cp₂TiCl-Promoted Isomerization of Trisubstituted Epoxides to *exo*-Methylene Allylic Alcohols on Carvone Derivatives. *J. Org. Chem.* **2004**, *69*, 5275-5280.
- (10) Pérez Morales, C.; Catalán, J.; Domingo, V.; González Delgado, J. A.; Dobado, J. A.; Mar Harrador, M.; Quílez del Moral, J.; Barrero, A. F. Protecting-Group-Free Synthesis of Chokols. *J. Org. Chem.* **2011**, *76*, 2494-2501.
- (11) Wielstra, Y.; Gambarotta, S.; Meetsma, A. The Controversy over the Thermal Stability of Bis(cyclopentadienyl)zirconium(III) Halides. Synthesis of Cp'₂ZrX (Cp' = Cp, C₅H₄M; X = Cl, Br, I) via Photolysis of Cp'₂Zr(*i*-Bu)X. The X-ray Structures of [(C₅H₄Me)₂Zr(μ-I)]₂ and [η⁵-η⁵-C₁₀H₈][CpZr(μ-I)]₂ *Organometallics* **1989**, *8*, 2948-2952.
- (12) Barr, K. J.; Watson, B. T.; Buchwald, S. L. Zirconocene (*iso*-butyl) Chloride: *In Situ* Generation of a Zirconocene(methyl) Chloride Equivalent for Use in Organic Synthesis. *Tetrahedron Lett.* **1991**, *32*, 5465-5468.

- (13) Justicia, J.; Jimenez, T.; Morcillo, S. P.; Cuerva, J. M.; Oltra, J. E. Mixed disproportionation versus radical trapping in titanocene(III)-promoted epoxide openings. *Tetrahedron* **2009**, *65*, 10837-10841.
- (14) Cuerva, J. M.; Campaña, A. G.; Justicia, J.; Rosales, A.; Oller-López, J. L.; Robles, R.; Cárdenas, D. J.; Buñuel, E.; Oltra, J. E. Water: The Ideal Hydrogen-Atom Source in Free-Radical Chemistry Mediated by Ti^{III} and Other Single-Electron-Transfer Metals? *Angew. Chem. Int. Ed.* **2006**, *45*, 5522-5526.
- (15) Barrero, A. F.; Oltra, J. E.; Cuerva, J. M.; Rosales, A. Effects of Solvent and Water in Ti(III)-Mediated Radical Cyclizations of Epoxygermacrolides. Straightforward Synthesis and Absolute Stereochemistry of (+)-3 α -Hydroxyreynosin and Related Eudesmanolides. *J. Org. Chem.* **2002**, *67*, 2566-2571.
- (16) Ahlrichs, R.; Armbruster, K. M.; Bär, M.; Baron, H.-P.; Bauernschmitt, R.; Crawford, N.; Deglmann, P.; Ehrig, M.; Eichkorn, K.; Elliott, S.; Furche, F.; Haase, F.; Häser, M.; Hättig, C.; Hellweg, A.; Horn, H.; Huber, C.; Huniar, U.; Kattannek, M.; Kölmel, C.; Kollwitz, M.; May, K.; Nava, P.; Ochsenfeld, C.; Öhm, H.; Patzelt, H.; Rappoport, D.; Rubner, O.; Schäfer, A.; Schneider, U.; Sierka, M.; Treutler, O.; Unterreiner, B.; von Arnim, M.; Weigend, F.; Weis, P.; Weiss, H. TURBOMOLE 7.0, Universität Karlsruhe: Karlsruhe, Germany, **2015**. See also <http://www.turbomole.com>.
- (17) Tao, J.; Perdew, J.; Staroverov, V.; Scuseria, G. Climbing the density functional ladder: Nonempirical meta-generalized gradient approximation designed for molecules and solids. *Phys. Rev. Lett.* **2003**, *91*, 146401/1-146401/4.
- (18) Weigend, F.; Ahlrichs, R. Balanced basis sets of split-valence, triple zeta valence and quadruple zeta valence quality for H to Rn: Design and assessment of accuracy. *Phys. Chem. Chem. Phys.* **2005**, *7*, 3297–3305.
- (19) Eichkorn, K.; Treutler, O.; Öhm, H.; Häser, M.; Ahlrichs, R. Auxiliary basis sets to approximate Coulomb potentials. *Chem. Phys. Lett.* **1995**, *242*, 652–660.
- (20) Weigend, F. Accurate Coulomb-fitting basis sets for H to Rn. *Phys. Chem. Chem. Phys.* **2006**, *8*, 1057–1065.
- (21) Grimme, S.; Antony, J.; Ehrlich, S.; Krieg, H. A consistent and accurate ab initio parameterization of density functional dispersion correction (DFT-D) for the 94 elements H-Pu. *J. Chem. Phys.* **2010**, *132*, 154104/1-154104/19.
- (22) (a) Grimme, S.; Ehrlich, S.; Goerigk, L. Effect of damping function in dispersion corrected density functional theory. *J. Comput. Chem.* **2011**, *32*, 1456–1465. (b) Becke, A. D.; Johnson, E. R. A density-functional model of the dispersion interaction. *J. Chem. Phys.* **2005**, *123*, 154101. (c) E. R. Johnson, E. R.; Becke, A. D. A post-Hartree-Fock model of intermolecular interactions. *J. Chem. Phys.* **2005**, *123*, 024101.
- (23) (a) Grimme, S.; Antony, J.; Schwabe, T.; Mück-Lichtenfeld, C. Density functional theory with dispersion corrections for supramolecular structures, aggregates, and complexes of

- (bio)organic molecules. *Org. Biomol. Chem.* **2007**, *5*, 741–758. (b) Grimme, S. Density functional theory with London dispersion corrections. *Wiley Interdisciplinary Reviews: Comput. Mol. Sci.* **2011**, *1*, 211–228.
- (24) (a) Zhang, Y.-Q.; Vogelsang, E.; Qu, Z.-W.; Grimme, S.; Gansäuer, A. Titanocene-Catalyzed Radical Opening of *N*-Acyated Aziridines. *Angew. Chem. Int. Ed.* **2017**, *56*, 12654–12657. (b) Schwarz G. Henriques, D.; Zimmer, K.; Klare, S.; Meyer, A.; Rojo-Wiechel, E.; Bauer, M.; Sure, R.; Grimme, S.; Schiemann, O.; Flowers, R. A. II; Gansäuer, A. Highly Active Titanocene Catalysts for Epoxide Hydrosilylation: Synthesis, Theory, Kinetics, EPR Spectroscopy. *Angew. Chem. Int. Ed.* **2016**, *55*, 7671–7675. (c) Gansäuer, A.; Kube, A. C.; Daasbjerg, K.; Sure, R.; Grimme, S.; Fianu, G. D.; Sadasivam, D. V.; Flowers, R. A. II Substituent Effects and Supramolecular Interactions of Titanocene(III) Chloride: Implications for Catalysis in Single Electron Steps. *J. Am. Chem. Soc.* **2014**, *136*, 1663–1671. (d) Grimme, S.; Kruse, H.; Goerigk, L.; Erker, G. The Mechanism of Dihydrogen Activation by Frustrated Lewis Pairs Revisited. *Angew. Chem. Int. Ed.* **2010**, *49*, 1402–1405. (e) Schwabe, T.; Grimme, S.; Djukic, J.-P. Noncovalent Metal-Metal Interactions: The Crucial Role of London Dispersion in a Bimetallic Indenyl System. *J. Am. Chem. Soc.* **2009**, *131*, 14156–14157.
- (25) Grimme, S. Supramolecular Binding Thermodynamics by Dispersion Corrected Density Functional Theory. *Chem. Eur. J.* **2012**, *18*, 9955–9964.
- (26) (a) Klamt, A. Conductor-like Screening Model for Real Solvents: A New Approach to the Quantitative Calculation of Solvation Phenomena. *J. Chem. Phys.* **1995**, *99*, 2224–2235. (b) Eckert, F.; Klamt, A. Fast solvent screening via quantum chemistry: COSMO-RS approach. *AIChE J.* **2002**, *48*, 369–385.
- (27) Eckert, F.; Klamt, A. J.; Pohler, L. COSMOtherm, Version C3.0, Release 14.01, COSMOlogic GmbH & Co. KG, Leverkusen, Germany, **2013**.
- (28) (a) Becke, A. D. Density functional exchange energy approximation with correct asymptotic behavior. *Phys. Rev. A* **1988**, *38*, 3098–3100. (b) Perdew, J. P. Density-functional approximation for the correlation energy of the inhomogeneous electron gas. *Phys. Rev. B* **1986**, *33*, 8822–8824.
- (29) Schäfer, A.; Huber, C.; Ahlrichs, R. Fully optimized contracted Gaussian basis sets of triple zeta valence quality for atoms Li to Kr. *J. Chem. Phys.* **1994**, *100*, 5829–5835.
- (30) Zhao, Y.; Truhlar, D. G. Design of Density Functions that Are Broadly Accurate for Thermochemistry, Thermochemical Kinetics, and Nonbonded Interactions. *J. Phys. Chem. A* **2005**, *109*, 5656–5667.
- (31) Becke, A. D. Density-functional thermochemistry III: The role of exact exchange. *J. Chem. Phys.* **1993**, *98*, 5648–5652. (b) Stephens, P. J.; Devlin, J.; Chabalowski, C. F.; Frisch, M. J. Ab Initio Calculation of Vibrational Absorption and Circular Dichroism Spectra Using Density Functional Force Fields. *J. Phys. Chem.* **1994**, *98*, 11623–11627.

APPENDIX: Cartesian Coordinates of Optimized Structures

Listed are the Cartesian coordinates of the optimized structures. Energies refer to the TPSS-D3/def2-TZVP level of theory and are given in au.

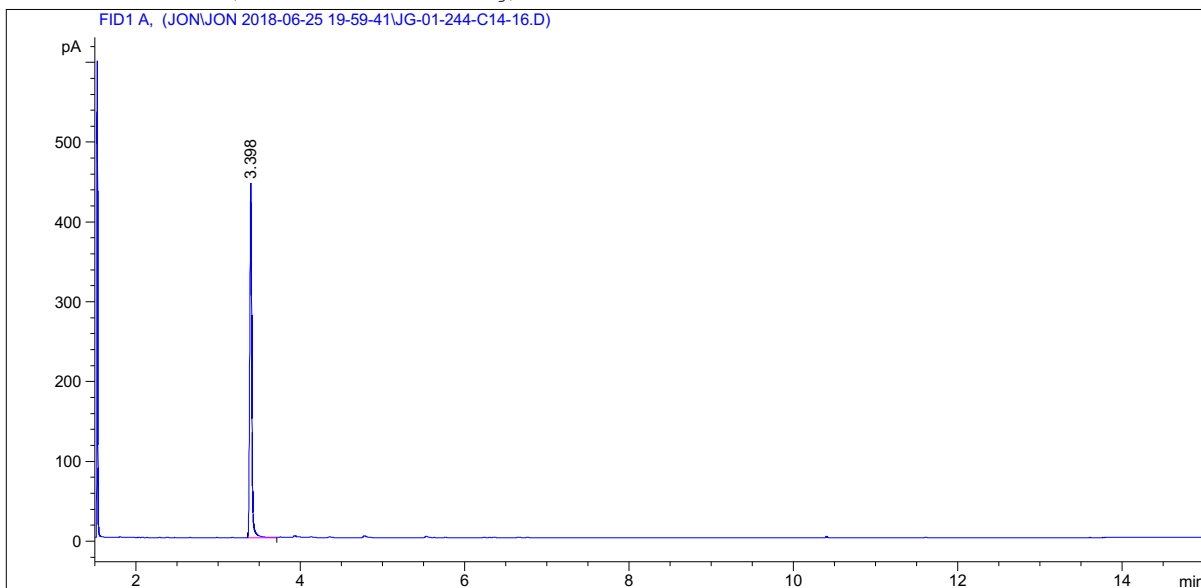
(This data is provided as an .xyz file which can be found among Supporting Information files)

SUPPORTING DATA: GC, GC-MS and EXPANDED NMR TRACES

Figure S11. Table 4, Entry 1. Chromatogram of authentic *cis*-10

Data File C:\CHEM32\1\DATA\JON\JON 2018-06-25 19-59-41\JG-01-244-C14-16.D
Sample Name: JG-01-244-c14-16

```
=====
Acq. Operator   : Jon                               Seq. Line :    1
Acq. Instrument : Instrument 1                       Location  : Vial 10
Injection Date  : 6/25/2018 8:02:47 PM              Inj       :    1
                                                    Inj Volume: 1 µl
Acq. Method     : C:\CHEM32\1\DATA\JON\JON 2018-06-25 19-59-41\60-RAMP-Q.M
Last changed    : 12/27/2017 4:32:54 PM by Jon
Analysis Method : C:\CHEM32\1\METHODS\COOL.M
Last changed    : 6/25/2018 10:08:37 PM by GRAY
                (modified after loading)
=====
```



Area Percent Report

```
Sorted By      :      Signal
Multiplier:    :      1.0000
Dilution:      :      1.0000
Use Multiplier & Dilution Factor with ISTDs
```

Signal 1: FID1 A,

Peak #	RetTime [min]	Type	Width [min]	Area [pA*s]	Height [pA]	Area %
1	3.398	BB	0.0277	786.96082	444.27094	93.47233
2	15.158	VV	0.0679	54.95763	11.17217	6.52767

Totals : 841.91845 455.44311

Figure S12. Table 4, Entry 1. ¹H NMR of authentic *cis*-10 in CDCl₃

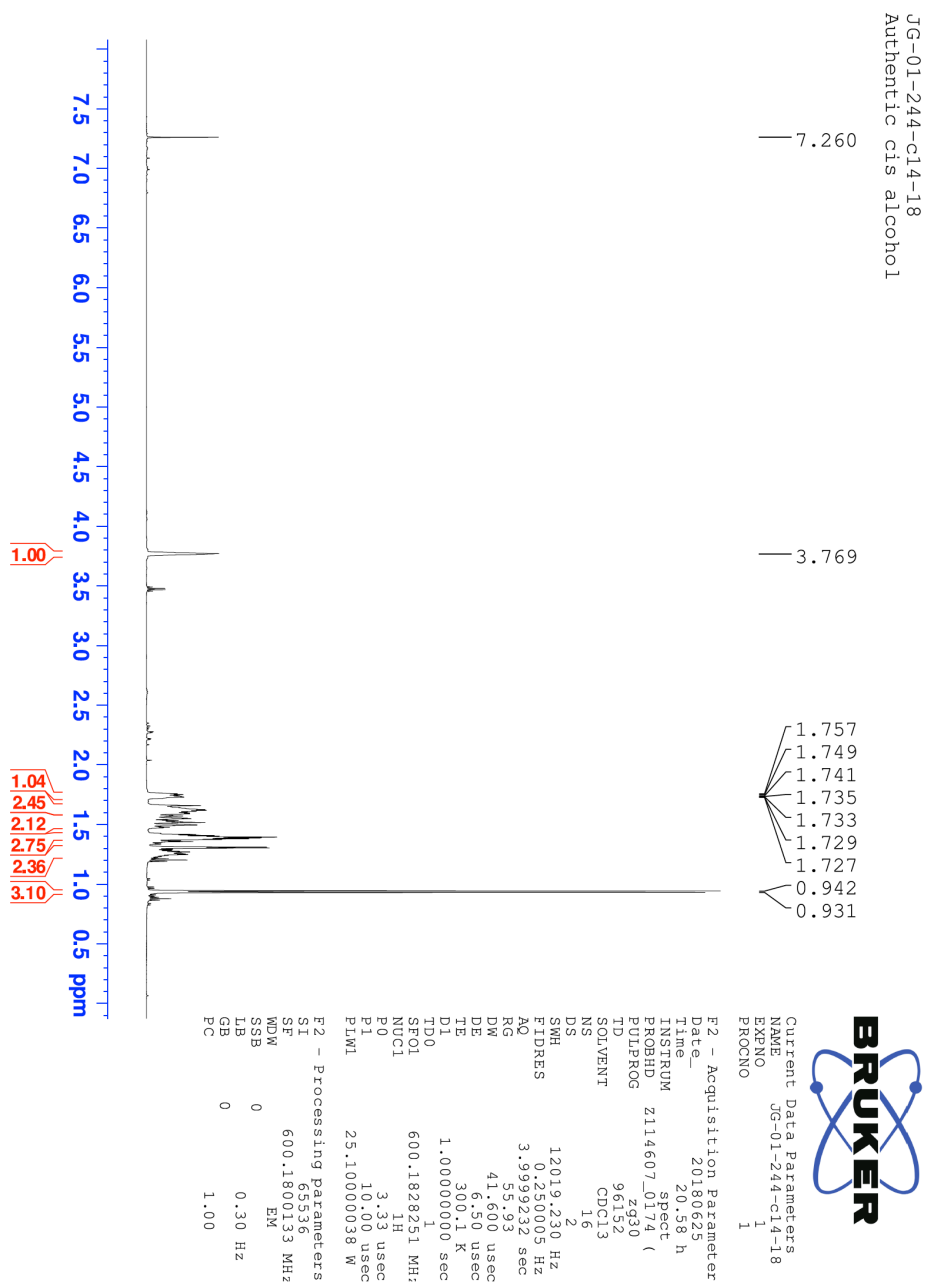
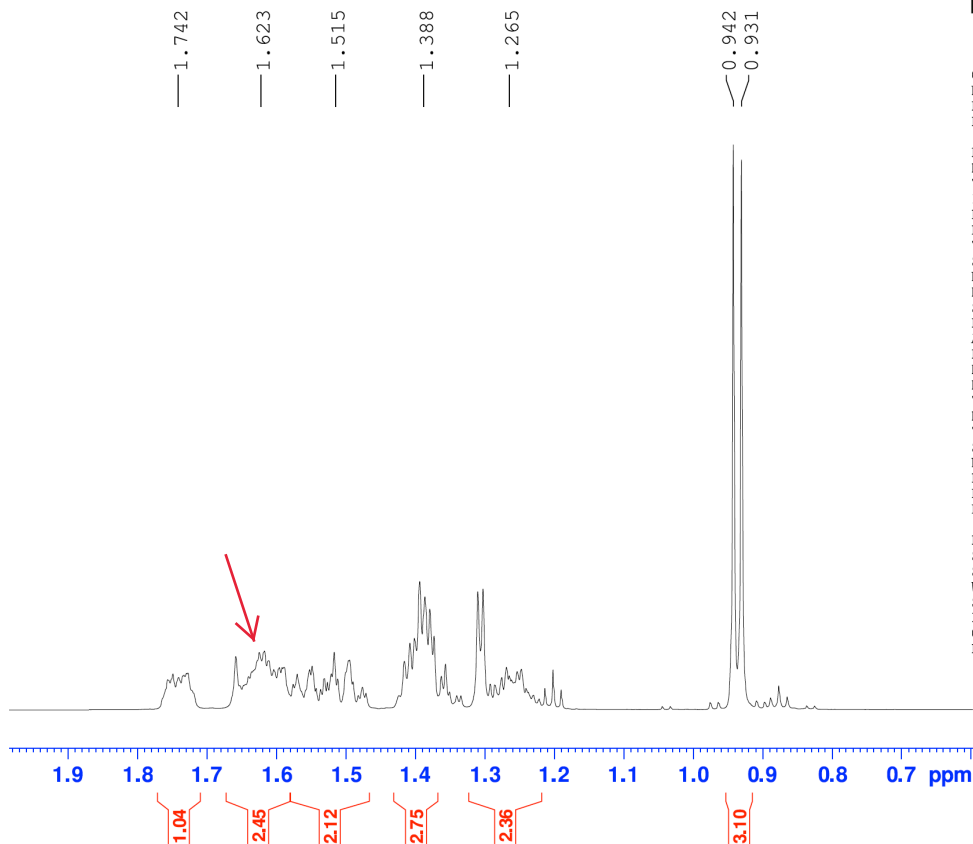


Figure S13. Table 4, Entry 1. ¹H NMR of authentic *cis*-10 (in CDCl₃ Expanded)

JG-244-c14-16 (isolated *cis* alcohol from authentic reduction sample)

JG-01-294-c14-18
Authentic *cis* alcohol



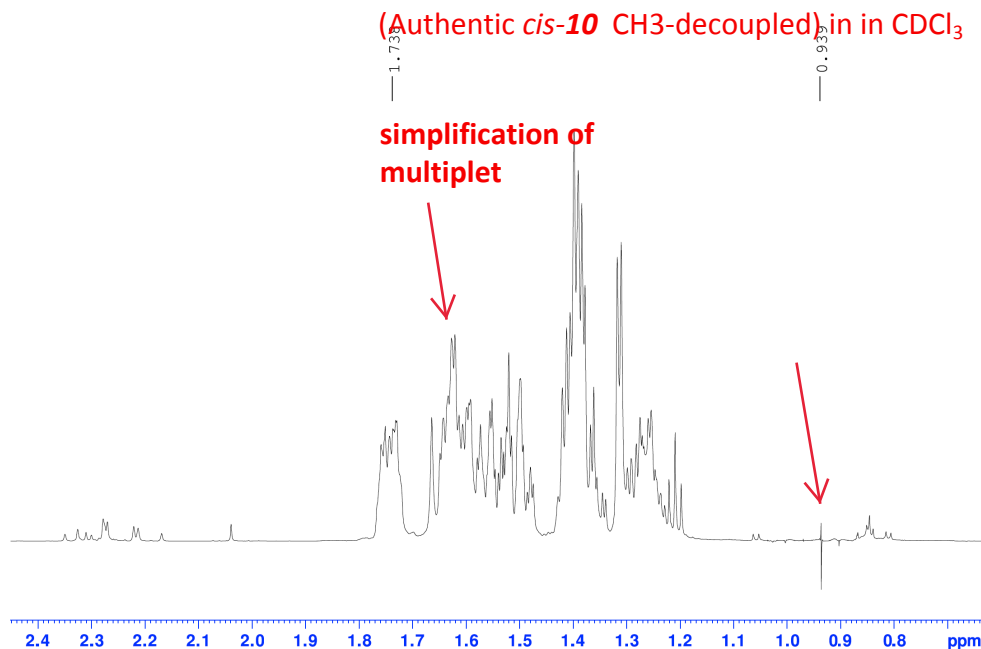
Current Data Parameters
 NAME JG-01-244-c14-18
 EXPNO 1
 PROCNO 1

F2 - Acquisition Parameter
 Date_ 20180625
 Time 20.58 h
 INSTRUM spect
 PROBHD Z114607_0174 (
 PULPROG zg30
 TD 96152
 SOLVENT CDCl3
 NS 16
 DS 2
 SWH 12019.230 Hz
 FIDRES 0.250005 Hz
 AQ 3.9999232 sec
 RG 55.93
 DW 41.600 usec
 DE 6.50 usec
 TE 300.1 K
 D1 1.00000000 sec
 TD0 1
 SF01 600.1828251 MHz
 NUC1 1H
 P0 3.33 usec
 P1 10.00 usec
 PLW1 25.10000038 W

F2 - Processing parameters
 SI 65536
 SF 600.1800133 MHz
 WDW EM
 SSB 0
 LB 0.30 Hz
 GB 0
 PC 1.00

Figure S14. JG-244-c14-16 (isolated *cis* alcohol decoupling of CH₃ doublet)

JG-01-244-c14-18-decoupling 1H
(irradiation of CH₃ doublet)



File :D:\MSDChemData\Babu\Jon\JG-01-244-3.D
Operator : Jon
Acquired : 12 Mar 2018 12:12 using AcqMethod 35-RAMP-5-JG.M
Instrument : GCMS
Sample Name: JG-01-244-3.D
Misc Info :
Vial Number: 1

Figure S15. Table 4, Entry 1. GC MS of authentic *cis*- and *trans*-10

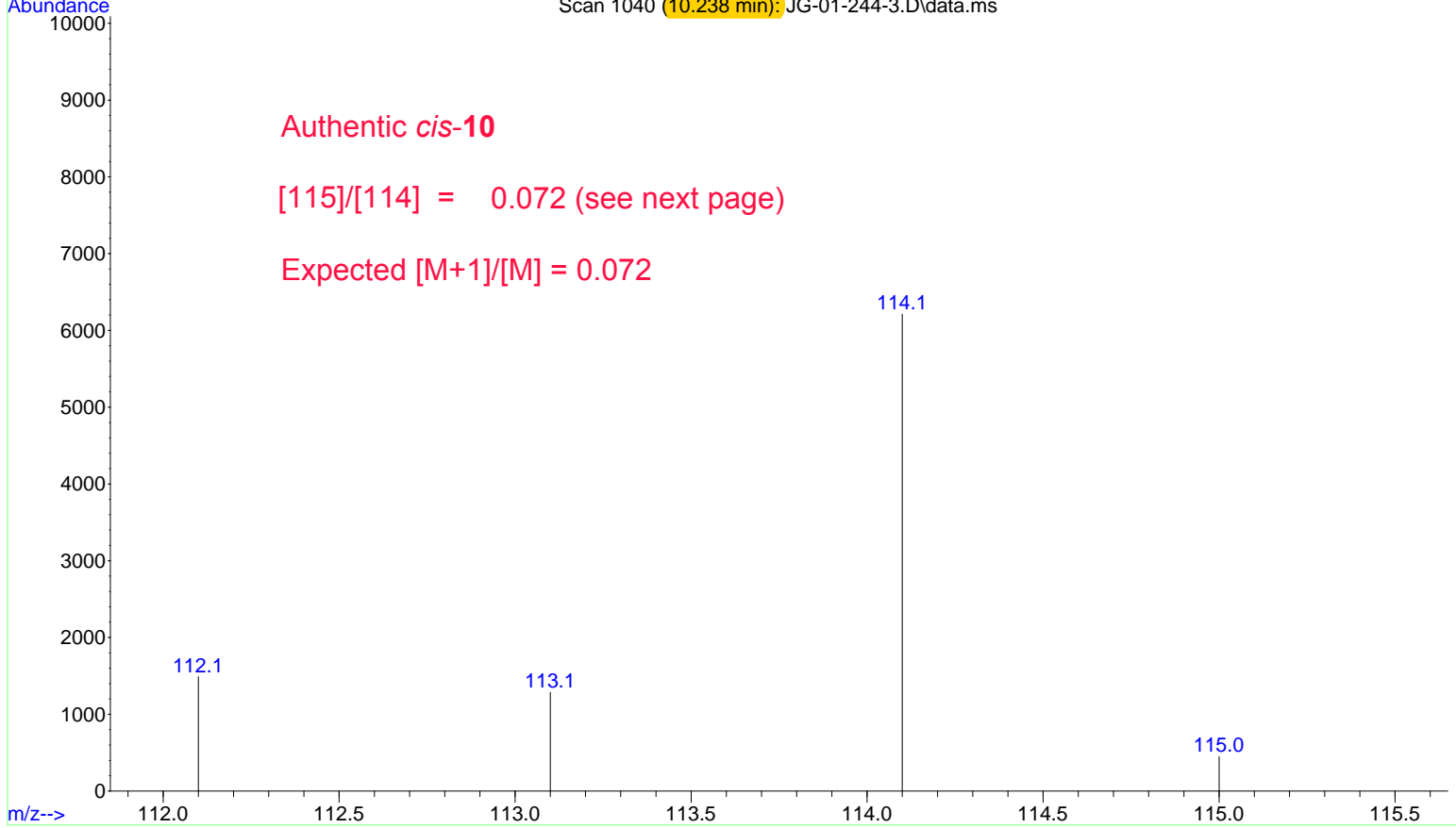
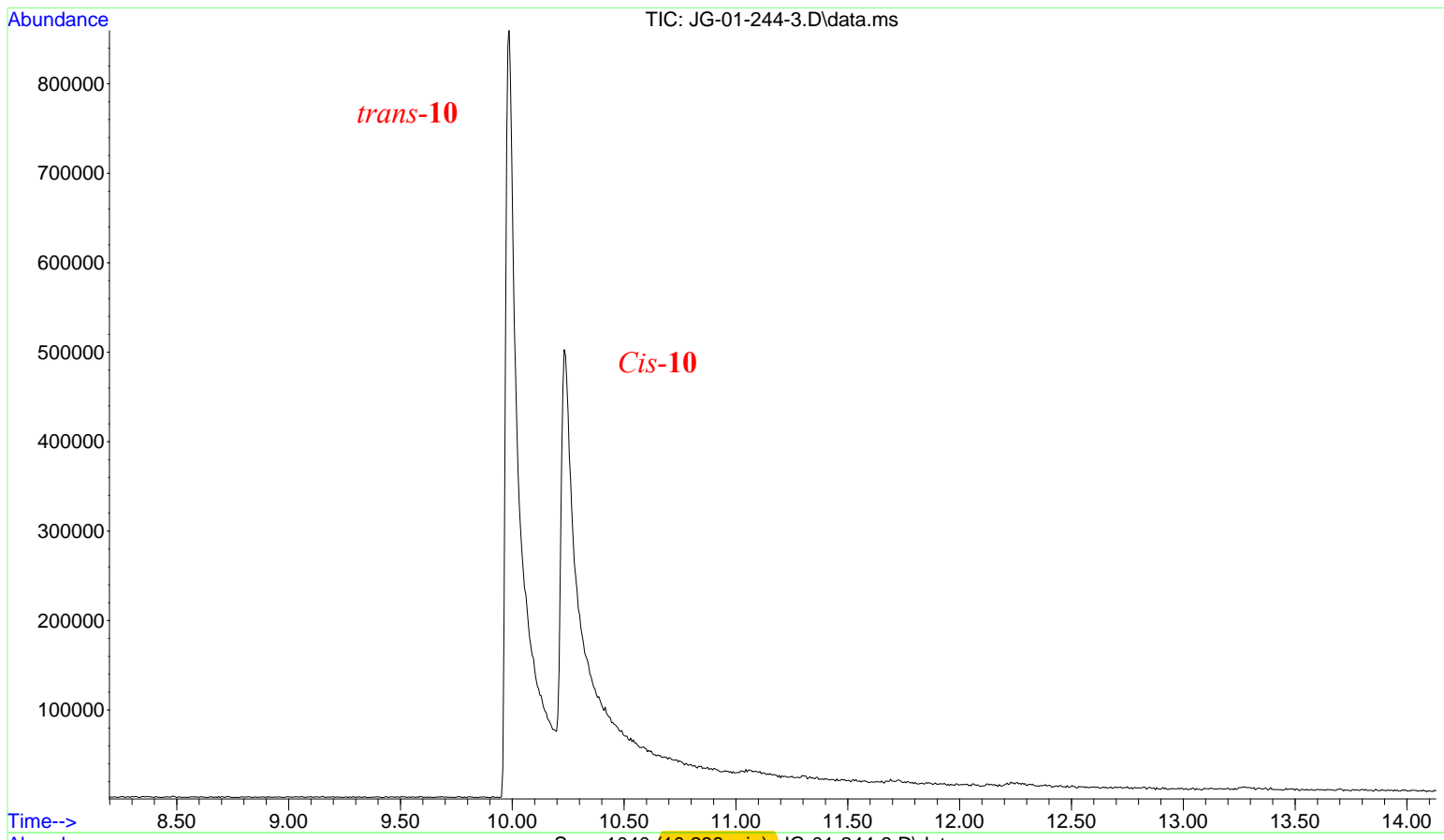


Figure S16. Table 4, Entry 1. GC MS of authentic *cis*-10

m/z	Abundance
51.00	2404.0
52.00	1013.0
53.10	7777.0
54.00	12024.0
55.10	29560.0
56.00	6783.0
57.00	75768.0
58.00	14164.0
59.00	854.0
62.00	339.0
63.10	656.0
65.00	2075.0
66.10	2843.0
67.10	23144.0
68.10	61952.0
69.00	7376.0
70.10	11398.0
71.10	40368.0
72.00	6451.0
73.00	863.0
73.90	216.0
77.00	2615.0
78.10	417.0
79.00	5357.0
80.00	1147.0
81.10	75448.0
82.00	5924.0
83.10	3409.0
84.10	1488.0
85.10	7155.0
86.10	7594.0
87.10	585.0
91.10	1196.0
91.80	237.0
93.00	581.0
94.10	498.0
95.00	5640.0
96.10	50312.0
97.10	4823.0
97.90	206.0
99.00	1836.0
112.10	1490.0
113.10	1287.0
114.10	6213.0
115.00	449.0
145.00	406.0
195.00	623.0
206.90	547.0
213.90	693.0

[M+1]/[M]= [115]/[114] 0.072

[small 116 (M+2), too small to measure]

Figure S17. Table 4, Entry 2. *cis*-10 prepared using Coll.HCl in THF-d8

m/z	Abundance
51.00	2827.0
52.00	1069.0
53.10	8169.0
54.00	12126.0
55.10	34400.0
56.10	6966.0
57.00	75760.0
58.00	12535.0
59.10	1128.0
62.00	438.0
63.00	755.0
64.10	228.0
65.10	2298.0
66.10	2405.0
67.10	24984.0
68.10	63408.0
69.00	8228.0
70.10	11888.0
71.10	42696.0
72.10	7193.0
73.10	852.0
73.90	271.0
77.00	2341.0
77.90	675.0
79.10	6122.0
80.20	1058.0
81.10	79536.0
82.10	6335.0
83.10	3801.0
84.00	2010.0
85.00	7150.0
86.10	7141.0
87.00	555.0
91.10	844.0
91.90	207.0
93.00	554.0
94.10	451.0
95.10	5205.0
96.10	55192.0
97.10	5803.0
98.00	248.0
99.00	1621.0
100.00	278.0
112.10	2175.0
113.10	1516.0
114.10	6276.0
115.10	545.0
207.00	1062.0
208.00	177.0

$$[M+1]/[M] = 115]/[114] = 0.087$$

[small 116, too small to measure]

File :D:\MSDCHEMData\Babu\Jon\JG-294-C13-15-D.D
Operator : Jon
Acquired : 21 Jul 2018 12:56 using AcqMethod 35-RAMP-5-JG.M
Instrument : GCMS
Sample Name: JG-294-C13-15-D
Misc Info :
Vial Number: 1

Figure S18. Table 4, Entry 3. *cis*-10 prepared using Coll.DCl in THF

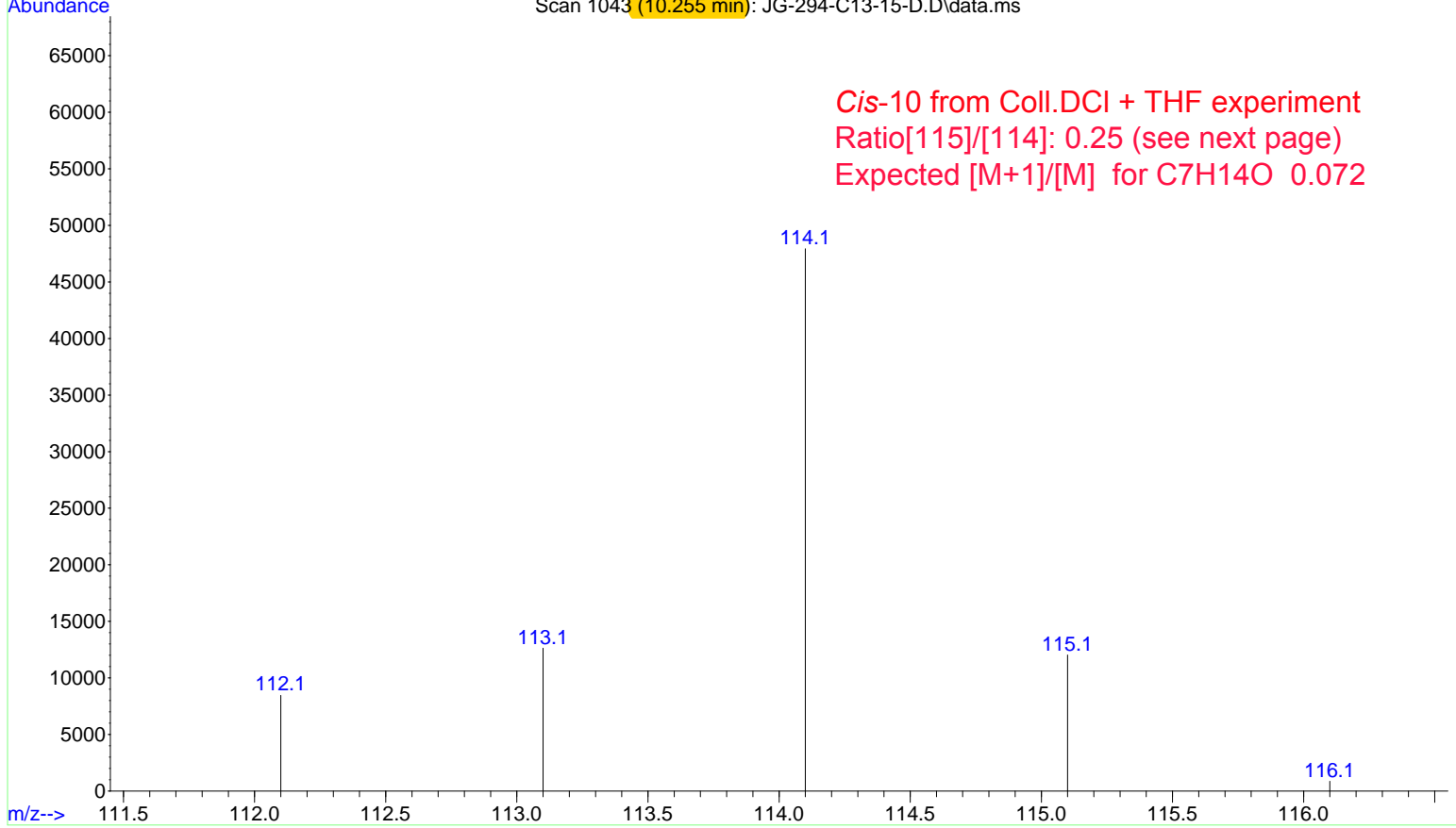
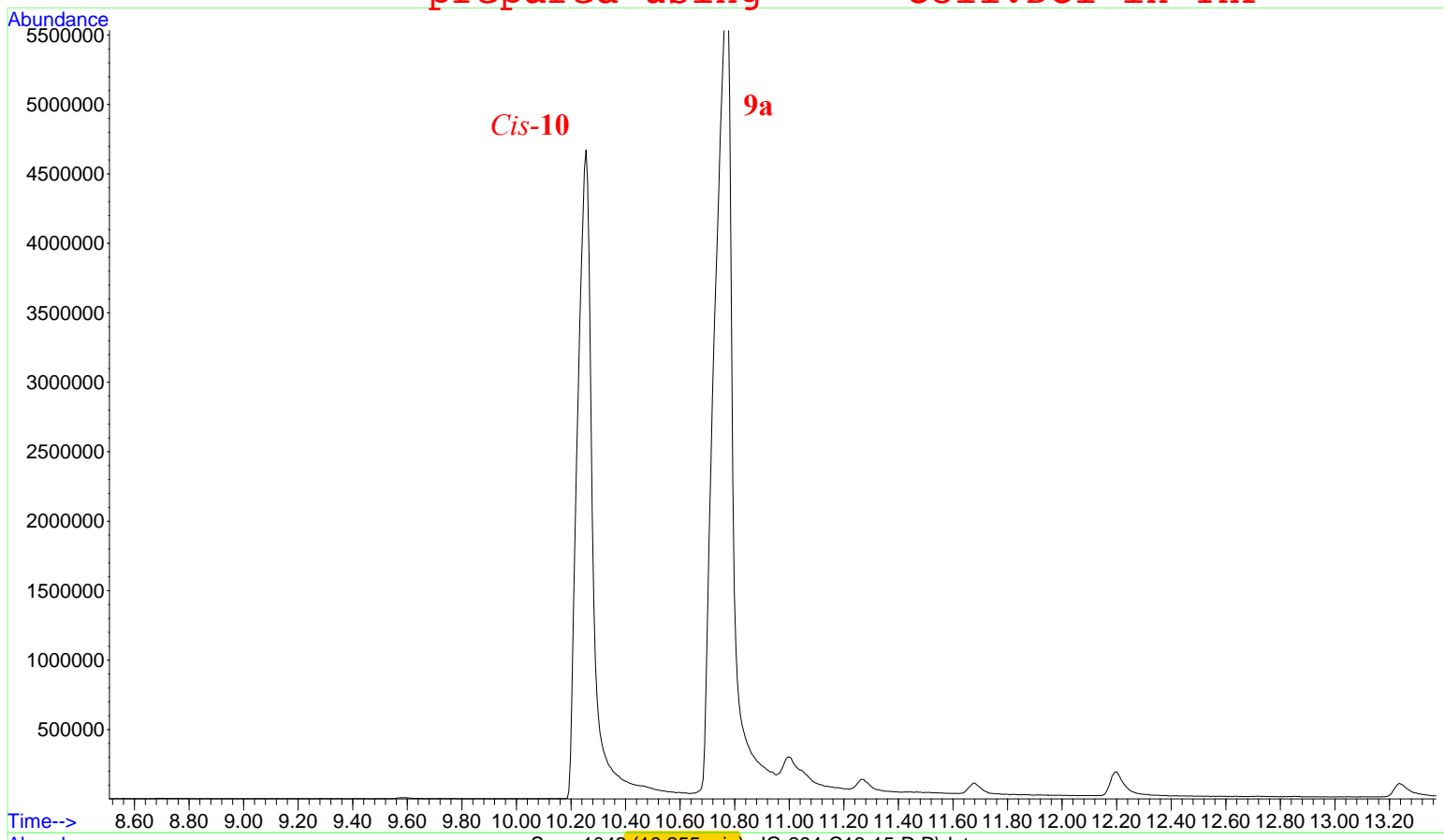


Figure S19. Stable 4, Entry 3. *cis*-10 prepared using Coll.DCl in THF

m/z	Abundance
50.10	11874.0
51.10	26696.0
52.10	11142.0
53.10	69560.0
54.10	102880.0
55.10	271680.0
56.10	82680.0
57.10	686912.0
58.10	131584.0
59.10	20400.0
60.00	1087.0
61.00	1285.0
62.10	2767.0
63.10	6900.0
64.10	1679.0
65.10	20768.0
66.10	22880.0
67.10	201536.0
68.10	513216.0
69.10	128152.0
70.10	100232.0
71.10	379456.0
72.10	72512.0
73.10	10179.0
74.00	1738.0
75.10	684.0
76.20	600.0
77.10	20632.0
78.00	5796.0
79.10	46904.0
80.10	14157.0
81.10	652480.0
82.10	142720.0
83.10	36168.0
84.10	13537.0
85.10	65600.0
86.10	65144.0
87.10	10299.0
88.10	662.0
89.10	440.0
90.20	211.0
91.10	6069.0
92.10	1211.0
93.10	4720.0
94.20	2134.0
95.10	44152.0
96.10	430656.0
97.10	116976.0
98.10	8130.0
99.10	14738.0
100.10	3092.0
100.90	256.0
107.10	262.0
110.00	510.0
111.10	462.0
112.10	8461.0
113.10	12625.0
114.10	47936.0
115.10	12033.0
116.10	865.0
145.10	203.0
207.00	853.0
207.90	161.0
281.00	323.0

$$[M+1]/[M] = [115]/[114] = 0.25$$

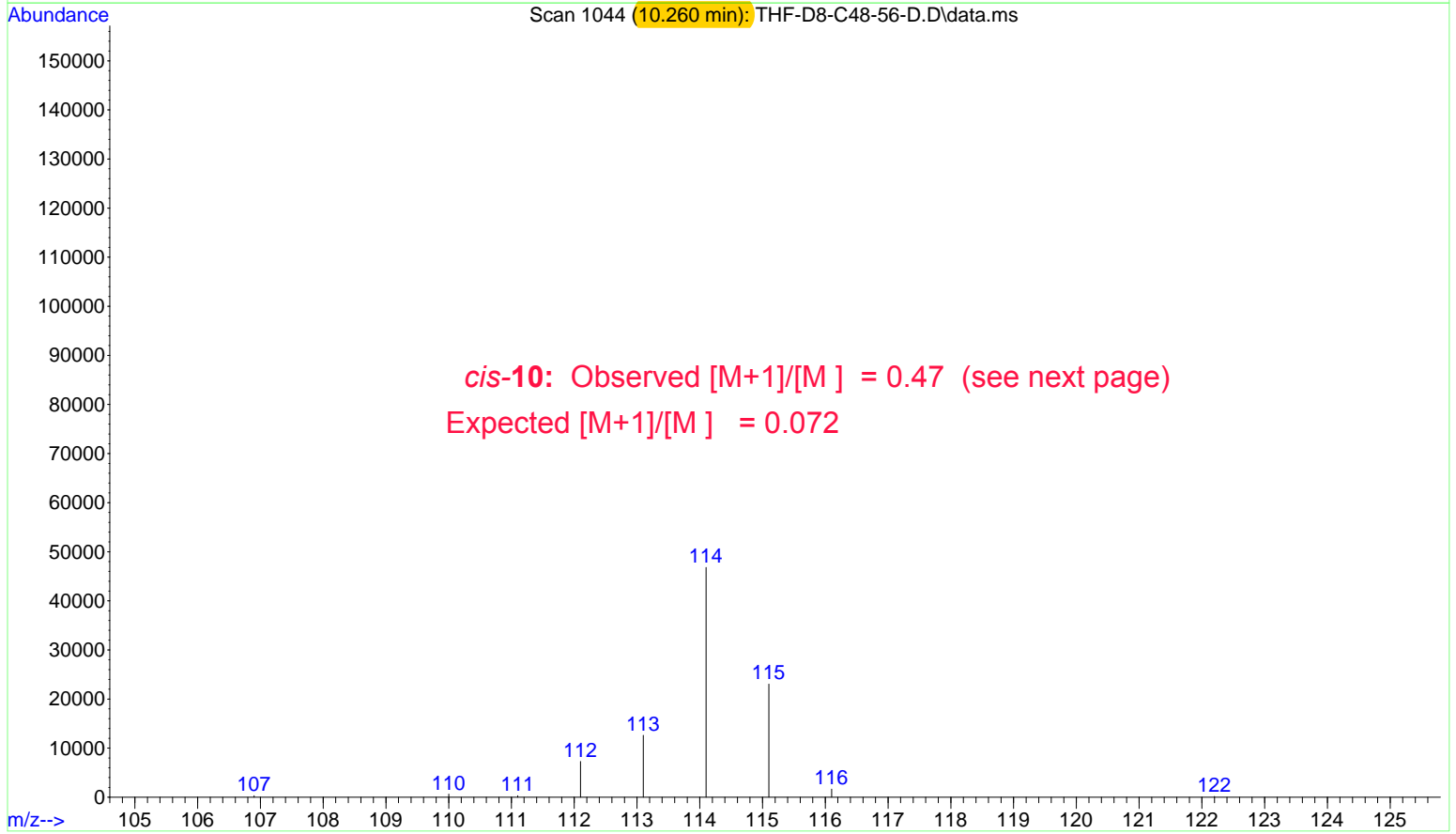
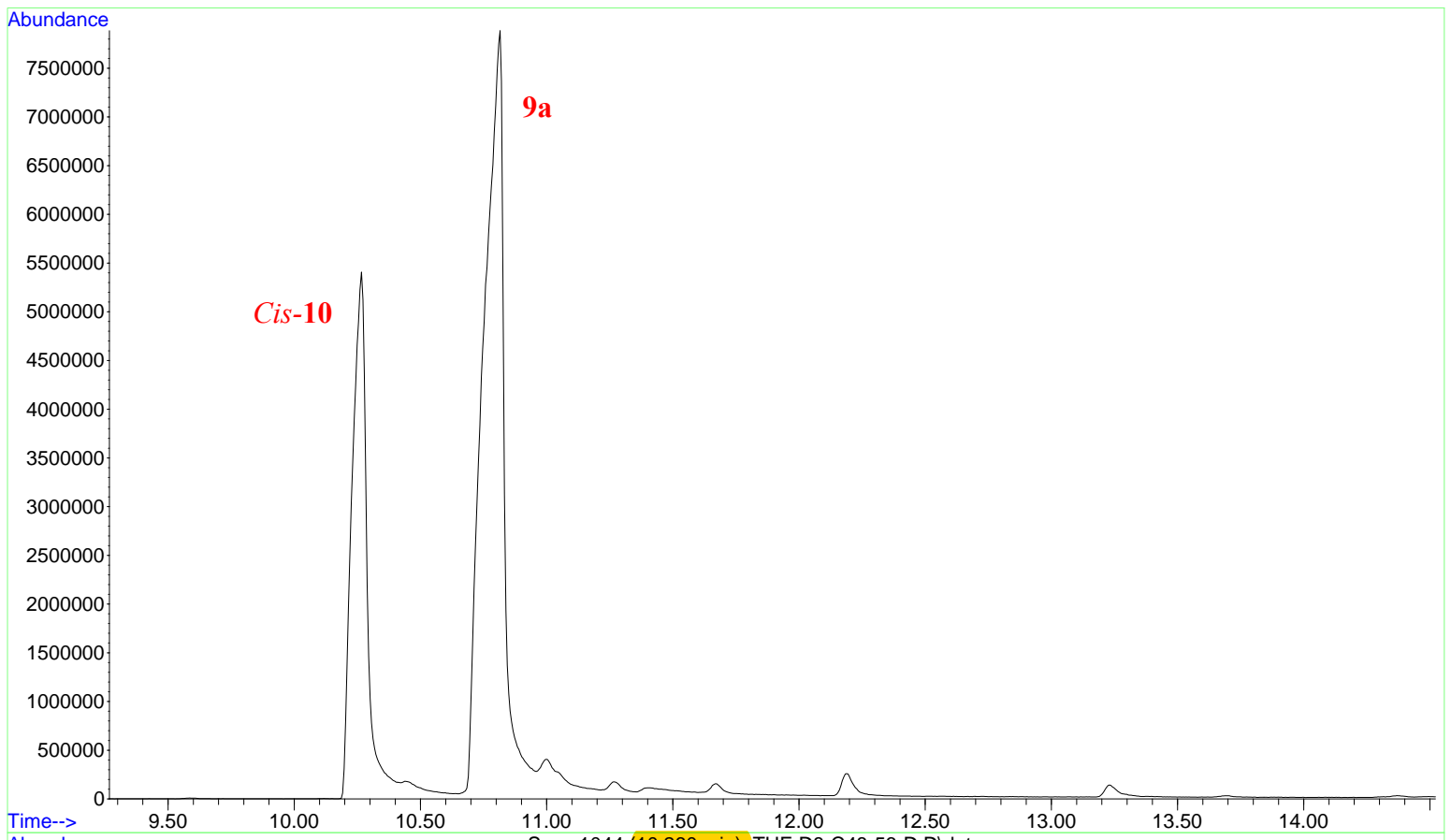
$$[M+2]/M+1] = [116/115] = 0.071$$

observed: $[M+1]/[M] = 0.25$; Expected 0.072

observed $[M+2]/[M+1] = 0.071$; Expected $[M+2]/[M+1] = 0.072$

File :D:\MSDCHEMData\Babu\Jon\THF-D8-C48-56-D.D
Operator : Jon
Acquired : 21 Jul 2018 13:55 using AcqMethod 35-RAMP-5-JG.M
Instrument : GCMS
Sample Name: THF-D8-C48-56-D
Misc Info :
Vial Number: 2

Figure S20. Table 4, Entry 4. cis-10 prepared using Coll.DCl in THF-d8



cis-10: Observed [M+1]/[M] = 0.47 (see next page)
Expected [M+1]/[M] = 0.072

**Figure S21. Table 4, Entry 4. *cis*-10
prepared using Coll.DCl in THF-d8
(Experiment 1)**

m/z	Abundance
50.10	14075.0
51.10	27688.0
52.10	12682.0
53.10	75688.0
54.10	115408.0
55.10	295168.0
56.10	113568.0
57.10	785984.0
58.10	160768.0
59.10	31416.0
60.00	2360.0
61.00	1179.0
62.00	3635.0
63.00	7616.0
64.10	2205.0
65.10	20704.0
66.10	27288.0
67.10	222464.0
68.10	557696.0
69.10	197888.0
70.10	107976.0
71.10	431040.0
72.10	88640.0
73.10	15848.0
74.00	2764.0
75.10	970.0
77.10	21624.0
78.10	8245.0
79.10	47568.0
80.10	20480.0
81.10	668096.0
82.10	251904.0
83.10	44696.0
84.10	15247.0
85.10	69672.0
86.10	78208.0
87.10	18856.0
88.20	1009.0
88.90	409.0
91.10	6931.0
92.10	2038.0
93.10	4414.0
94.10	3248.0
95.10	45680.0
96.10	443008.0
97.10	201088.0
98.10	15554.0
99.10	13097.0
100.10	5299.0
101.10	321.0
106.90	337.0
108.90	162.0
110.00	469.0
110.90	640.0
112.10	8070.0
113.10	13741.0
114.10	49952.0
115.10	22232.0
116.10	1768.0
190.90	156.0
207.00	734.0
208.10	195.0

$$[M+1]/[M+] = [115]/[114] = 0.45$$

$$[M+2]/[M+1] = [116/115] = 0.079$$

Expected $[M+1]/[M] = 0.072$; Observed = 0.45

Expected $[M+2]/[M+1] = 0.072$; observed = 0.079

Figure S22. Table 4, Entry 4. *cis*-10
prepared using Coll.DCl in THF-d8
(Experiment 2)

m/z	Abundance
50.10	2584.0
51.10	5439.0
52.10	2542.0
53.10	14657.0
54.10	23000.0
55.10	56888.0
56.10	20240.0
57.10	145152.0
58.10	30208.0
59.10	5598.0
60.10	383.0
60.90	253.0
61.90	579.0
63.00	1290.0
64.10	479.0
65.10	4175.0
66.10	5290.0
67.10	40712.0
68.10	102384.0
69.10	35656.0
70.10	21360.0
71.10	78968.0
72.10	16152.0
73.10	2941.0
74.10	459.0
75.00	176.0
77.10	3516.0
78.00	1483.0
79.10	8377.0
80.10	4172.0
81.10	120496.0
82.10	46352.0
83.10	8715.0
84.10	3116.0
85.10	12918.0
86.10	14370.0
87.10	3335.0
87.90	179.0
91.00	1131.0
92.10	457.0
93.10	766.0
94.10	686.0
95.10	7577.0
96.10	79944.0
97.10	34816.0
98.10	2824.0
99.10	2149.0
100.00	863.0
111.10	209.0
112.10	2407.0
113.20	2633.0
114.10	8612.0
115.10	4038.0
116.00	313.0
207.00	704.0

[115]/[114] 0.47

[116/115] 0.078

Expected [M+1]/[M] = 0.072; observed = 0.47

Expected [M+2]/[M+1] = 0.072; observed = 0.078

m/z	Abundance
51.00	6774.0
52.00	2431.0
53.00	19432.0
54.00	31808.0
55.00	83400.0
56.00	18440.0
57.00	204800.0
58.00	34032.0
59.00	3568.0
59.90	171.0
61.00	292.0
61.90	989.0
63.00	1889.0
64.10	260.0
65.00	5336.0
66.00	6616.0
67.00	62208.0
68.00	160256.0
69.00	20728.0
70.00	30232.0
71.00	113656.0
72.00	18848.0
73.00	1818.0
73.90	564.0
75.00	249.0
77.00	6357.0
78.00	1590.0
79.00	13984.0
80.00	2511.0
81.00	200640.0
82.00	15936.0
83.00	13058.0
84.00	3689.0
85.00	19504.0
86.00	18080.0
86.90	1358.0
87.90	205.0
91.00	1884.0
91.90	388.0
93.00	1263.0
94.00	913.0
95.00	14198.0
96.00	134720.0
97.00	13318.0
98.00	776.0
99.00	4430.0
99.90	365.0
101.00	230.0
111.00	234.0
112.00	4162.0
113.00	3770.0
114.00	13869.0
115.00	944.0
206.90	1130.0
207.80	396.0
281.00	530.0

Figure S23. *cis*-10 from STOICHIOMETRIC REACTION in THF-d8 (1 equiv Cp2TICl, no collidine)

Very little D incorporation

$M+1/M = [115]/[114] = 0.068$ Expected 0.072

$M+2/M+1$ [116]-too small to measure